



Calhoun: The NPS Institutional Archive
DSpace Repository

Theses and Dissertations

1. Thesis and Dissertation Collection, all items

1967-09

A comparison of four non-divergent wind fields

Brodehl, Richard Brian

Monterey, California. U.S. Naval Postgraduate School

<http://hdl.handle.net/10945/11802>

This publication is a work of the U.S. Government as defined in Title 17, United States Code, Section 101. Copyright protection is not available for this work in the United States.

Downloaded from NPS Archive: Calhoun



Calhoun is the Naval Postgraduate School's public access digital repository for research materials and institutional publications created by the NPS community. Calhoun is named for Professor of Mathematics Guy K. Calhoun, NPS's first appointed -- and published -- scholarly author.

Dudley Knox Library / Naval Postgraduate School
411 Dyer Road / 1 University Circle
Monterey, California USA 93943

<http://www.nps.edu/library>

NPS ARCHIVE
1967
BRODEHL, R.

A COMPARISON OF FOUR
NON-DIVERGENT WIND FIELDS

RICHARD BRIAN BRODEHL

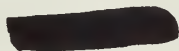
1
2

1
2

A COMPARISON OF FOUR NON-DIVERGENT WIND FIELDS

by

Richard Brian Brodehl
Lieutenant, United States Navy
B.S. , Naval Academy, 1962



Submitted in partial fulfillment of the
requirements for the degree of

MASTER OF SCIENCE IN METEOROLOGY

from the

NAVAL POSTGRADUATE SCHOOL
September 1967

NPS ARCHIVE
1967
BRODEHL, R.

~~100315~~
B 8092340-
C.1

ABSTRACT

This paper is concerned with the comparison of four different non-divergent wind fields obtained from a single geopotential height field over a dense data area. After developing the divergence equation of the non-divergent stream function, four different stream functions are obtained by modification and/or deletion from the basic equation. Isotach patterns for each stream function are computed. A comparison of the four stream function patterns and their corresponding isotach patterns is made. Two of the stream functions are used to obtain the non-divergent wind field for the initial wind conditions in a primitive equation model developed by Krishnamurti. Two 36-hour forecasts are made. A comparison of the forecasts is made at three-hour intervals up to 24 hours and at 36 hours. Both forecasts are compared to the reported winds at 12-hour intervals.

TABLE OF CONTENTS

<u>Section</u>	<u>Page</u>
1. INTRODUCTION	9
2. DEVELOPMENT OF THE NON-DIVERGENT WIND EQUATIONS	11
3. PROCEDURES	14
4. DISCUSSION OF WIND FIELD COMPARISONS	15
5. THE NUMERICAL FORECASTS	17
6. DISCUSSION OF RESULTS OF THE FORECASTS	19
7. BIBLIOGRAPHY	24

LIST OF ILLUSTRATIONS

<u>Figure</u>		<u>Page</u>
1.	13 April 1964, 1200Z, 200mb. geopotential height contours	25
2.	13 April 1964, 1200Z, 200mb. ψ_L contours	26
3.	13 April 1964, 1200Z, 200mb. ψ_{N1} contours	27
4.	13 April 1964, 1200Z, 200mb. ψ_{N2} contours	28
5.	13 April 1964, 1200Z, 200mb. V_g isotachs	29
6.	13 April 1964, 1200Z, 200mb. V_{ψ_L} isotachs	30
7.	13 April 1964, 1200Z, 200mb. $V_{\psi_{N1}}$ isotachs	31
8.	13 April 1964, 1200Z, 200mb. $V_{\psi_{N2}}$ isotachs	32
9.	13 April 1964, 1200Z, 200mb. reported winds	33
10.	Graph of $V_{(\)}$ versus Latitude for line "A" in Figures 1, 5, 6, 7 and 8	34
11.	Graph of $V_{(\)}$ versus Latitude for line "B" in Figures 1, 5, 6, 7 and 8	35
12.	Graph of $V_{(\)}$ versus Latitude for line "C" in Figures 1, 5, 6, 7 and 8	36
13.	Table of comparison of $V_{(\)}$ and reported winds	37
14.	12 April 1964, 0000Z, 200mb. height contours	38
15.	12 April 1964, 0000Z, 200mb. V_g isotachs	39
16.	12 April 1964, 0000Z, 200mb. isotachs of reported winds	40
17.	U and V at 3 hours for V_g and $V_{\psi_{N2}}$	41
18.	U and V at 6 hours for V_g and $V_{\psi_{N2}}$	42

<u>Figure</u>		<u>Page</u>
19.	U and V at 9 hours for V_g and $V_{\psi_{N2}}$	43
20.	U and V at 12 hours for V_g and $V_{\psi_{N2}}$	44
21.	U and V at 15 hours for V_g and $V_{\psi_{N2}}$	45
22.	U and V at 18 hours for V_g and $V_{\psi_{N2}}$	46
23.	U and V at 21 hours for V_g and $V_{\psi_{N2}}$	47
24.	U and V at 24 hours for V_g and $V_{\psi_{N2}}$	48
25.	U and V at 36 hours for V_g and $V_{\psi_{N2}}$	49
26.	Reported winds and prognostic U + V fields of V_g and $V_{\psi_{N2}}$ for 1200Z, 12 April 1964	50
27.	Reported winds and prognostic U + V fields of V_g and $V_{\psi_{N2}}$ for 0000Z, 13 April 1964	51
28.	Reported winds and prognostic U + V fields of V_g and $V_{\psi_{N2}}$ for 1200Z, 13 April 1964	52
29.	Table of comparison of reported winds and prognostic winds shown in Figures 26, 27 and 28	53

TABLE OF SYMBOLS

g	the gravitational acceleration
z	the height of an isobaric surface
Φ	the geopotential height, gz
f	the Coriolis parameter, $2\Omega \sin\phi$, where ϕ is the latitude
ψ	the stream function for the non-divergent wind
χ	the velocity potential for the divergent wind
w	the vertical velocity in pressure coordinates
∇	the del operator
∇^2	the Laplacian operator
J	the horizontal Jacobian operator, $J(A, B) = \frac{\partial A}{\partial x} \frac{\partial B}{\partial y} - \frac{\partial A}{\partial y} \frac{\partial B}{\partial x}$
V_g	the geostrophic wind
V_{ψ_L}	the linear balanced wind
$V_{\psi_{N1}}$	the semi-geostrophic balanced wind
$V_{\psi_{N2}}$	the complete balanced wind
u, U	the zonal component of velocity, + u is easterly
v, V	the meridional component of velocity, + v is northerly
ψ_g	the geostrophic stream function
ψ_L	the linear balanced stream function
ψ_{N1}	the semi-geostrophic stream function
ψ_{N2}	the complete balanced stream function
Z	GCT (Greenwich Central Time)

1. INTRODUCTION

It is now evident that the use of pure quasi-geostrophic equations of motion in numerical forecasting has reached a plateau. There is little evidence that they will be much more accurate as far as prognosis is concerned. W. Blumen (1) has given evidence of shortcomings in the quasi-geostrophic approximations. These are due to excessive non-linear "adjustment times" before pure geostrophic balance is reached. This balance is a requirement in all quasi-geostrophic models but has special significance in the non-linear baroclinic models. Charney (2) implies that although the quasi-geostrophic models, by eliminating the high frequency noise disturbances, have given us valuable insight to the physical properties of meteorological significant waves, they are only the beginning of a new era in numerical forecasting. He mentions the inherent errors of the geostrophic approximation and that further improvements in the models would only lead to highly complex methods which would tend to destroy the basic idea of the geostrophic approximation -- its simplicity. Charney suggests that the primitive Eulerian equations as first proposed by Richardson are the next step in successful numerical forecasting.

It is known that extremely accurate initial wind conditions are needed in order to successfully determine accelerations and divergence from the primitive equations; acceleration and divergence are an order

of magnitude smaller than the measurable quantities in the atmosphere (3). Use of the primitive equations will then depend on our ability to adequately describe an initial wind field that will: 1) be a close representation of the actual wind, 2) be compatible with numerical calculation as far as stability and time incrementation is concerned, and 3) be obtainable from present measured data. Charney (2) develops the "Balance" equation which is used to describe an initial wind field that meets the above criteria. (See Section 2 for this development).

Charney also considers the geostrophic wind components, u_g and v_g , as part of the initial wind conditions in the primitive equations. Through a numerical example he shows that large inertio-gravitational oscillations occur. These results show the existence and accumulation of large amounts of divergence, a characteristic of gravity waves but not of the meteorological significant waves.

In this paper the "Balance" equation is developed. Using various modifications of the equation, four different non-divergent stream functions are determined and compared with their isotach patterns. Using Krishnamurti's primitive equation model, two 36-hour forecasts are made, one with the initial winds being geostrophic (a modification of the "Balance" equation), and the other with initial winds determined from the unmodified "Balance" equation. The two forecasts will be compared at three-hour intervals up to 24 hours and at 36 hours. Both forecasts will be compared to reported winds at 12, 24 and 36 hours.

2. DEVELOPMENT OF THE NON-DIVERGENT WIND EQUATIONS

There were two approaches to the development of the non-divergent wind equation, henceforth called the "Balance" equation. Charney's approach (2) was that of necessity. He found that something better than the geostrophic approximation was needed in order to determine the initial wind fields for use in the primitive equations. Examining the actual divergence in the atmosphere, he noted that horizontal divergences were very small. Therefore, he said, the horizontal wind components can be described accurately as partial derivatives of a non-divergent stream function, ψ , as follows:

$$u = -\frac{\partial \psi}{\partial y} \quad v = \frac{\partial \psi}{\partial x} .$$

By placing these values into the divergence equation, then eliminating insignificant terms, Charney arrives at the "Balance" equation. He implies that since this equation is a representation of non-divergent winds, and since the inertio-gravitational winds are characterized by relatively large divergences, then the equation, if satisfied, will prohibit the occurrence of gravity waves. He mentions collaborators who have shown the same results and proved his implications.

A more sophisticated approach to the development is that of Thompson (5). His intention was to re-examine the filtering problem of the geostrophic approximation and to see if it could be improved by providing the filtering (elimination of gravity waves) with less

restrictions. To do this it was necessary to determine the feature of the equation of motion that generates the gravity waves, and then to eliminate this feature with some kind of filtering approximation. Thompson accomplishes this by obtaining the frequency equation of the linearized (by perturbation method) divergence equation. He determines that the roots of the frequency equation which correspond to gravity waves, are those due to the total derivative of the divergence in the divergence equation. By removing this total derivative there is eliminated the possibility of having any gravity waves when the modified divergence equation is satisfied. This modified equation is the "Balance" equation as determined by Charney.

From Helmholtz, velocity can be expressed as the sum of non-divergent and divergent parts:

$$V = kx \nabla \psi + \nabla \chi . \quad (2-1)$$

Starting with the horizontal equation of motion

$$\left. \frac{dV}{dt} \right|_H = -f kxV - \nabla \Phi , \quad (2-2)$$

the horizontal divergence equation is obtained:

$$\frac{\partial \nabla \cdot V}{\partial t} + \frac{u \partial (\nabla \cdot V)}{\partial x} + \frac{v \partial (\nabla \cdot V)}{\partial y} + \nabla u \cdot \frac{\partial V}{\partial x} + \nabla v \cdot \frac{\partial V}{\partial y} = -\nabla \cdot f kxV - \nabla^2 \Phi . \quad (2-3)$$

Removing the total derivative of horizontal divergence from (2-3) leaves,

$$\frac{\partial V}{\partial x} \cdot \nabla u + \frac{\partial V}{\partial y} \cdot \nabla v = -\nabla \cdot f kxV - \nabla^2 \Phi . \quad (2-4)$$

Substituting the following expressions into equation (2-4):

$$V = kx \nabla \psi \quad u = -\frac{\partial \psi}{\partial y} \quad v = \frac{\partial \psi}{\partial x} . \quad (2-5)$$

the "Balance" equation of the non-divergent wind is obtained:

$$\nabla \cdot f \nabla \psi = \nabla^2 \Phi - 2J \left[\frac{\partial \psi}{\partial x}, \frac{\partial \psi}{\partial y} \right]. \quad (2-6)$$

This equation defines the non-divergent wind from a height field, z , and eliminates inertio-gravitational waves as long as it is satisfied.

Using equation (2-6) Krishnamurti (4) develops expressions for the following four stream functions:

(1) ψ_g , the geostrophic stream function by dropping the non-linear term on the right side of (2-6) and treating the coriolis parameter, f , as a constant, giving

$$\nabla^2 \psi = \frac{1}{f_0} \nabla^2 \Phi \quad \text{or} \quad g = \frac{gz}{f_0},$$

(2) ψ_L , the linear balanced stream function by dropping the non-linear term and treating f as a variable, giving

$$\nabla^2 \psi = -\frac{1}{f} (\nabla \psi \cdot \nabla f) + \frac{1}{f} \nabla^2 \Phi,$$

(3) ψ_{N1} , the semi-geostrophic balanced stream function by evaluating the non-linear term using geostrophic wind components giving

$$\nabla^2 \psi = -\frac{1}{f} (\nabla \psi \cdot \nabla f) + \frac{1}{f} \nabla^2 \Phi - \frac{2J}{f} \left[u_g, v_g \right].$$

(4) ψ_{N2} , the complete balanced stream function by making no changes or assumptions in the "Balance" equation.

The numerical considerations of convergence in solving for the complete balanced stream function are discussed by Krishnamurti.(2-6).

Generally, the requirement for a convergent solution is that the equation be elliptic. This requirement is met if:

$$\nabla^2 \psi > \frac{f}{2}.$$

3. PROCEDURES

Using 200-mb data for 1200Z, 13 April 1964, an accurate geopotential height field (50 meter interval) was plotted within the following area: 25N to 60N, 70W to 135W. These contours represent the geostrophic stream function, ψ_g . Krishnamurti (4) uses this height field to compute the stream functions, ψ_L , ψ_{N1} , and ψ_{N2} . Figure 1 is the geopotential height field. Figures 2, 3 and 4 show the stream functions, ψ_L , ψ_{N1} and ψ_{N2} , respectively, plotted with the height contours on a polar stereographic projection. Stream function interval is $50 \times 10^5 \text{ m}^2 \text{ sec}^{-1}$.

Taking the expression for the non-divergent wind:

$$V = k \times \nabla \psi ,$$

wind speeds were computed at over 200 points in the fields of ψ_L , ψ_{N1} and ψ_{N2} , and isotachs were drawn. Isotachs of the geostrophic wind were drawn to speeds computed from:

$$V_g = k \times \frac{g}{f_0} \nabla z .$$

Figures 5 through 8 are the isotach fields of the four stream functions.

Three graphs of wind speed versus latitude were drawn. The first is along the line through the isotach maximums, labeled line "A"; the second along the 95th meridian, labeled line "B"; the third along the 115th meridian, labeled line "C". These graphs are Figures 10, 11 and 12 respectively.

Reported winds are shown in Figure 9. Figure 13 is a table comparing the reported winds to each of the four computed winds.

4. DISCUSSION OF WIND FIELD COMPARISONS

Examining the streamline patterns, Figures 2, 3 and 4, we see that definite cross-contour flow exists. Generally the flow is to lower heights upstream of close contour spacing and to higher heights where contours spread. The linear balanced stream function, being closest to the geostrophic wind in computational simplicity, exhibits the least cross-contour flow. The complete balanced stream function shows the most cross-contour flow and therefore corresponds more closely to statistical observations of this phenomenon (6). The flow exhibited by the non-linear stream functions is a direct manifestation of the theories on geostrophic adjustment (7).

Only the complete balanced stream function shows strong anti-cyclonic flow over New Orleans. This is the area of the sub-tropical jet stream. The anti-cyclonic flow seems to be excessive but may be due to boundary values in computations or a lack of data.

It must be remembered that the streamlines represent the non-divergent wind. The divergent parts of the wind are small. Krishnamurti says that calculations for this map time give divergent winds that are at no place greater than five percent of the total wind.

Streamline spacing corresponds well to contour spacing (geostrophic streamlines). This is reflected in the isotach patterns of Figures 5 through 8, and the three graphs, Figures 10, 11 and 12. The linear

balanced winds are close to geostrophic winds. Krishnamurti has shown (4) that at low levels where strong cyclonic and closed circulations exist, the linear balanced winds are far too large. At 200-mb the geostrophic wind maximum in the trough will approach the complete balanced wind when corrected for curvature. The semi-geostrophic balanced winds are close to the complete balanced winds. However, only the complete balanced winds give a good representation of the subtropical jet.

Figure 13 shows a numerical comparison of the computed and reported winds. The overall mean algebraic difference indicates that the balanced winds are closer to the reported winds than the geostrophic winds are. A comparison of this type at the 200-mb level must be viewed with caution. It is known that high values of vertical wind shear exist at this level. Small errors in balloon height can give unrepresentative reported winds. Looking at the isotach patterns of the computed winds, we also see large horizontal shears. In areas of high winds and large shears, the downwind position of the balloon from the reporting station could be in a sector of the computed wind isotach field that contains a velocity range of up to 20 knots. It would be very difficult to include the turning of the wind with height to get an accurate balloon position in order to compare the reported and computed wind at that point. It might be advantageous to make a smooth isotach analysis of the reported winds and use this to compare the computed winds. There still will exist, however, the problem of balloon location and which winds have errors.

Lacey (9) compared the geostrophic winds and the non-divergent complete balanced winds with the reported winds at 850-mb, 700-mb, 500-mb and 300-mb over the United States. His comparison was made for both direction and speed. He found that on the average the complete balanced winds were much closer to the reported winds in both direction and speed when the complete balanced wind and the geostrophic wind differed by more than five degrees or five knots. He also determined that adding the divergent winds to the non-divergent complete balanced winds produced little change in the non-divergent wind pattern. The divergent winds were about two to three percent of the total wind.

From the above discussion it can be concluded that the complete balanced wind is the most accurate description of the true wind. The question, "are the complete balanced winds accurate enough for use as initial wind conditions in the primitive equations?" will be discussed in the next section.

5. THE NUMERICAL FORECASTS

In the Introduction it was mentioned that Charney proposed balanced winds as sufficient initial conditions for numerical prognosis using the primitive equations. His main point was that the geostrophic wind did not filter the "noise" while the balanced winds did. He used a simple model to prove this point. However, Phillips (8) has shown that because Charney's model was too simple, he overlooked the fact that using only the non-divergent winds as initial conditions ($\nabla \cdot \mathbf{V} = 0$ at $t = 0$), the forecast using an actual baroclinic atmospheric model

would still contain considerable "noise". Phillips claims that the noise generated by the restriction to non-divergence could be eliminated by including the divergence obtained from geostrophic approximations in the initial data.

Krishnamurti has developed a primitive equation model in which he has incorporated the ideas of Charney, Phillips, Thompson and others. His initial wind field is a combination of the non-divergent wind determined from the "Balance" equation and the divergent wind obtained by computing divergence. Any combination of computing methods to calculate balanced winds and vertical motions (thus, divergence) can be used to determine the initial conditions. He has done extensive work on partitioning the atmosphere by using his model with initial conditions determined as follows:

- a. The non-divergent stream function, ψ_{N2} , by using the complete non-linear balance equation.
- b. Vertical velocity expressed in a complicated omega equation involving ψ_{N2} , and the divergent velocity potential, χ .
- c. The divergent velocity potential, χ , expressed in the manifestation of the continuity equation:

$$\nabla^2 \chi = -\frac{\partial}{\partial p} \frac{w}{p}.$$

From the initial conditions obtained in the above manner, a 36-hour forecast was obtained.

A much simpler procedure would be to use the quasi-geostrophic approximation in all phases of calculating the initial wind conditions. Though this approximation itself has proven to be inadequate if used

solely as the initial wind condition, one might ask that if it were combined with quasi-geostrophic divergence as suggested by Phillips, would it still be inadequate? A second forecast was made using Krishnamurti's model with the initial conditions determined as follows:

a. The non-divergent stream function, ψ_g , determined from the geostrophic approximation.

b. Vertical velocity expressed in the quasi-geostrophic omega equation.

c. The continuity equation expressed as:

$$\nabla^2 \chi_g = -\frac{\partial w}{\partial p}.$$

In both forecasts, grid distance was:

$$y = 2-1/2 \text{ degrees latitude,}$$

$$x = y \text{ sine latitude.}$$

The area covered was from 55W to 135W and from 25N to 60N. Time steps were ten minutes. North and south boundary conditions were fixed. The eastern boundary was extended eastward six grid distances and combined cyclically with a western boundary extended six grid distances westward. Data used were the height field from 0000Z, 12 April 1964. Figures 14, 15 and 16 show the contours, geostrophic wind isotachs, and reported wind isotachs, respectively.

6. DISCUSSION OF RESULTS OF THE FORECASTS

Figures 17 through 25 show the complete balanced and quasi-geostrophic component u and v fields at three-hour intervals up to 24 hours and at 36 hours, respectively. These figures yield the following observations:

a. At three hours (Figure 17) there are already considerable differences between the balanced and geostrophic components.

In the u field at 55N, 75W, there exists a negative 5 m-sec^{-1} center in the geostrophic field, but a positive 15 m-sec^{-1} in the balanced field. The elongated center on both over the northwestern United States is 15 m-sec^{-1} larger in the balanced field. The 50 m-sec^{-1} center off Washington in the balanced field is only 20 m-sec^{-1} in the geostrophic field and is displaced 15 to 20 degrees west. The sub-tropical jet over Florida is expressed well in the balanced field but is displaced south in the geostrophic field. Many irregularities appear in the geostrophic field while the balanced field exhibits a smooth, realistic pattern.

In the v fields there is much more agreement. This should be expected because of the fixed boundary values. We note that the positive area centered at 105W on both fields is much smaller in area and strength in the balanced field. The opposite is true for the negative area at 125W. A look at Figures 15 and 16 reveal that the balanced field is more realistic.

b. At six hours (Figure 18) the differences noted at three hours between balanced and geostrophic components are even more pronounced. There are now strong indications of inertio-gravitational oscillations in the geostrophic field. Looking at the u fields we notice that a large high latitude negative center extends the length of the chart in the geostrophic field, while the balanced field shows only a decrease in the positive zonal flow in the same area. The similarity over northwestern

United States which existed at three hours has almost disappeared even though the balanced field shows little change during the three hours.

The balanced field of the v component shows little change in three hours, but the geostrophic v field shows a great increase of negative components at higher latitudes. The overall similarity that existed at three hours is disappearing at six hours.

c. At nine hours (Figure 19) the balanced components are behaving well. There is a slight easterly progression of the u maximum at 130W, 45N, and the ridge line in the v field along the west coast has easterly movement. In the u field we see the sub-tropical jet maximum moving eastward.

The geostrophic u field has become strongly negative above 50N. The indication of a sub-tropical jet is becoming distorted, and it is becoming difficult to distinguish the developing trough. The v field now shows good continuity with the past three hours and is becoming similar to the balanced v field.

d. The balanced components show good continuity at 12 hours (Figure 20). The geostrophic u field is now rapidly losing the high latitude negative center that existed at nine hours. The geostrophic v field retains continuity but there is evidence of oscillations. The negative center at 125W is lagging the balanced negative center by about ten degrees.

e. The balanced components at 15 hours (Figure 21) still have good continuity and retain pattern shape. The geostrophic v field seems

to have settled down with a pattern development similar to the balanced field. The geostrophic u field has lost its negative values but still shows oscillations. This field has only half the positive velocity as the balanced u field, and no marked centers exist.

f. For 18 hours (Figure 22) and 21 hours (Figure 23) the same trends exist. The geostrophic u field has again established a negative area above 50N while the rest of the field bears little resemblance to the balanced one.

g. At 24 hours (Figure 24) the geostrophic u field has the negative area in high latitudes with no indication of a jet stream anywhere. The pattern slightly resembles the balanced pattern but the values are all much lower. The balanced u field appears to be developing strong positive values in the lower left corner. This may be due to the cyclic feed through from the lower right maximum which existed at the start of the forecast. The v fields show pattern similarity but the geostrophic field has a great predominance of positive values; the negative areas having small values.

h. The 36-hour prognostic u and v fields (Figure 25) show a pattern breakdown. The balanced u field has strong distortion from cyclic feed through, but maintains a resemblance of the synoptic situation in its pattern shape. The geostrophic u field shows strong distortion with a negative area undercutting a positive one. The balanced v field has distortion in the western half with weak centers indicating a very weak ridge. The geostrophic v field shows a counter-clockwise

rotation of the prevailing pattern in the western half, with a very strong negative center just east of Florida.

It can be concluded from the above discussion that the quasi-geostrophic approximation, even by including divergence, is unstable and gives rise to large inertio-gravitational oscillations when used for initial conditions in the primitive equations. From the limitations and boundary values applied in this model, the conclusion is most evident in the u component field.

A further comparison of the prognoses was made by comparing the reported wind speeds to the prognostic winds. Prognostic winds were obtained by vector addition of the u and v fields. Figures 26, 27 and 28 show the reported winds and the prognostic balanced and geostrophic winds at 12, 24 and 36 hours, respectively. The table of Figure 29 shows definitely that the balanced winds are much better than the geostrophic winds for the 12 and 24-hour prognoses. At 36 hours too much distortion and cyclic feed through exist to make a reliable comparison, for the geostrophic prognosis appears to be better.

The major conclusion in this numerical forecast comparison is that the balanced winds give the prognosis a wind pattern that resembles the synoptic situation. The geostrophic winds gave rise to considerable large-scale "noise" and unrealistic patterns.

7. BIBLIOGRAPHY

- (1) Blumen, W. "On Nonlinear Geostrophic Adjustment," J. Atmospheric Sciences, Vol. 24, 1967. pp 325-332.
- (2) Charney, J. "The Use of the Primitive Equations of Motion in Numerical Prediction," Tellus, Vol. 7, 1955. pp 22-26.
- (3) Haltiner, George J. and Frank L. Martin. Dynamical and Physical Meteorology. New York: McGraw-Hill, 1957. Chapter 22.
- (4) Krishnamurti, T. N., Julia Nogues and Dave Baumhefner. On the Partitioning Of the Baroclinic Vertical Motions In a Developing Wave Cyclone. Air Force Cambridge Research Laboratory (AFCRL 66-419), Contract No. AF 19(629)-4777, May 1966.
- (5) Thompson, Philip D. Numerical Weather Analysis and Prediction. New York: The MacMillan Company, 1961. Chapter II.
- (6) Simis, H. The Relation of the Jet Stream Axis to Contour Direction. Canadian Circular 3018, 21 February 1958.
- (7) Bolin, B. "The Adjustment of a Non-balanced Velocity Field Toward Geostrophic Equilibrium in a Stratified Fluid," Tellus, Vol. 5, 1953. pp 373-385.
- (8) Phillips, Norman A. "On the Problem of Initial Data for the Primitive Equations," Tellus, Vol. 12, 1960. pp 121-126.
- (9) Lacy, Fred Ernst. A Comparison of Numerically Determined Divergent and Non-divergent Winds to Geostrophic Winds. Thesis L167, Naval Postgraduate School, Monterey, California, 1964.

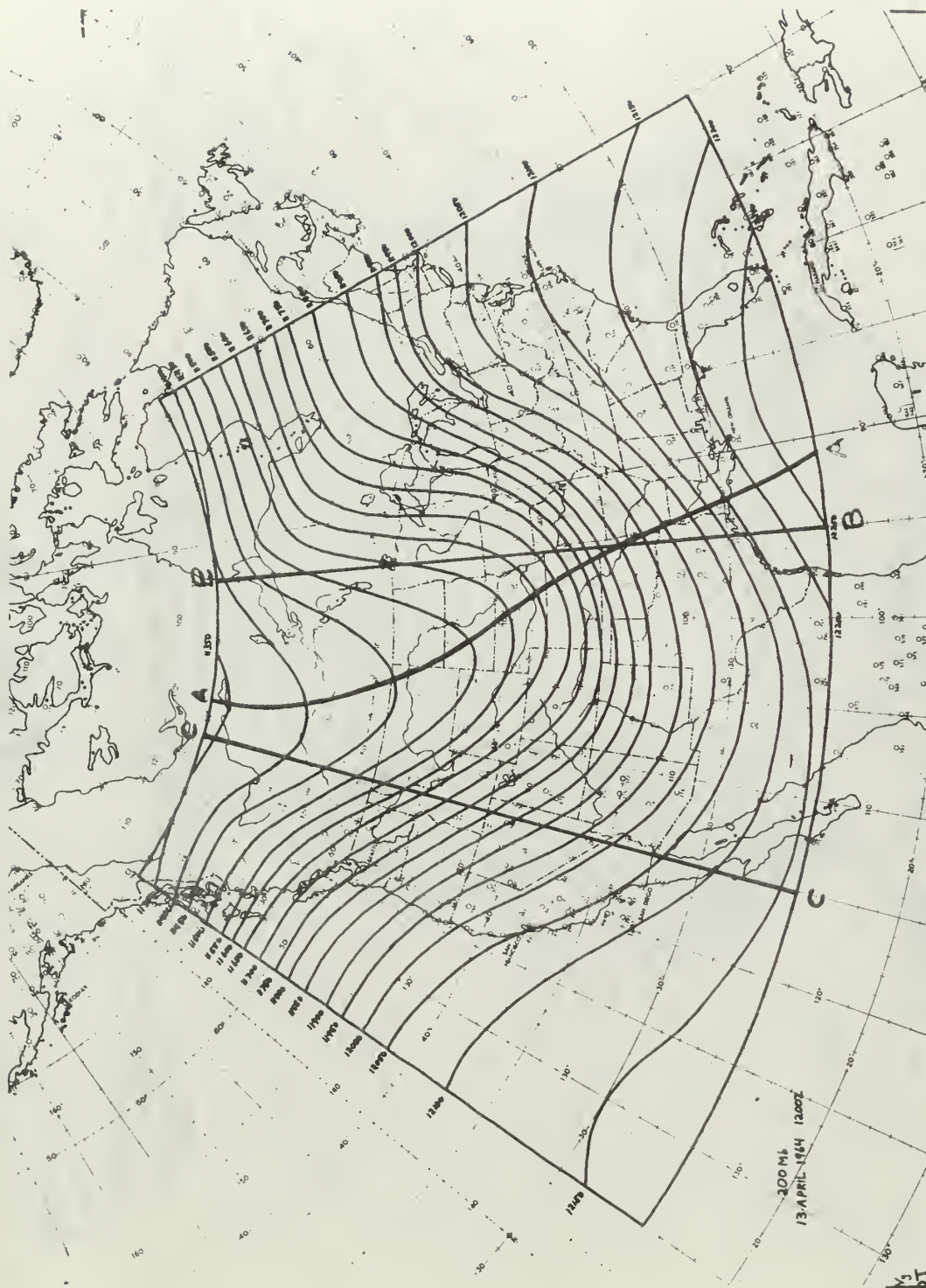


FIG. 1

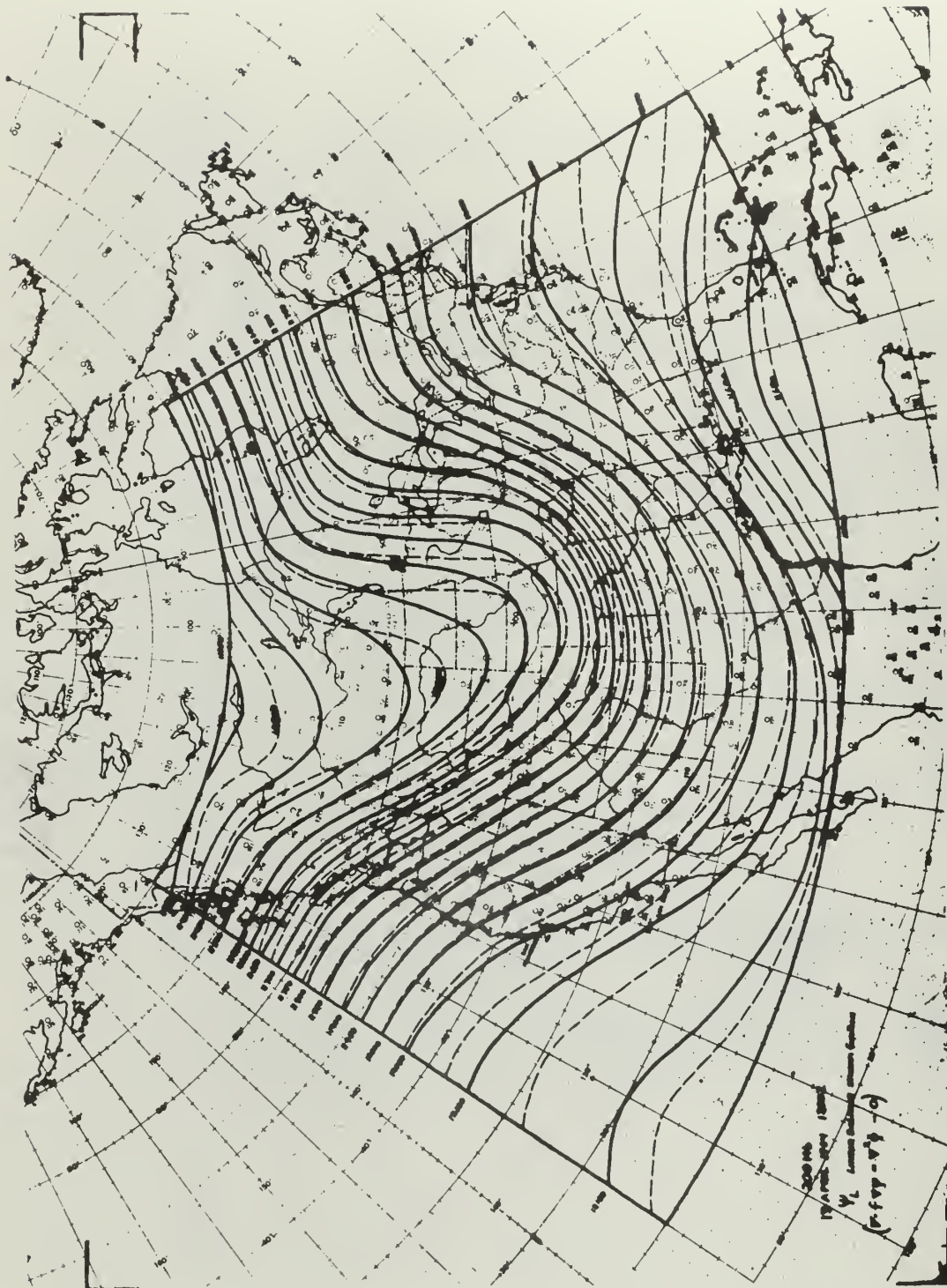


FIG. 2

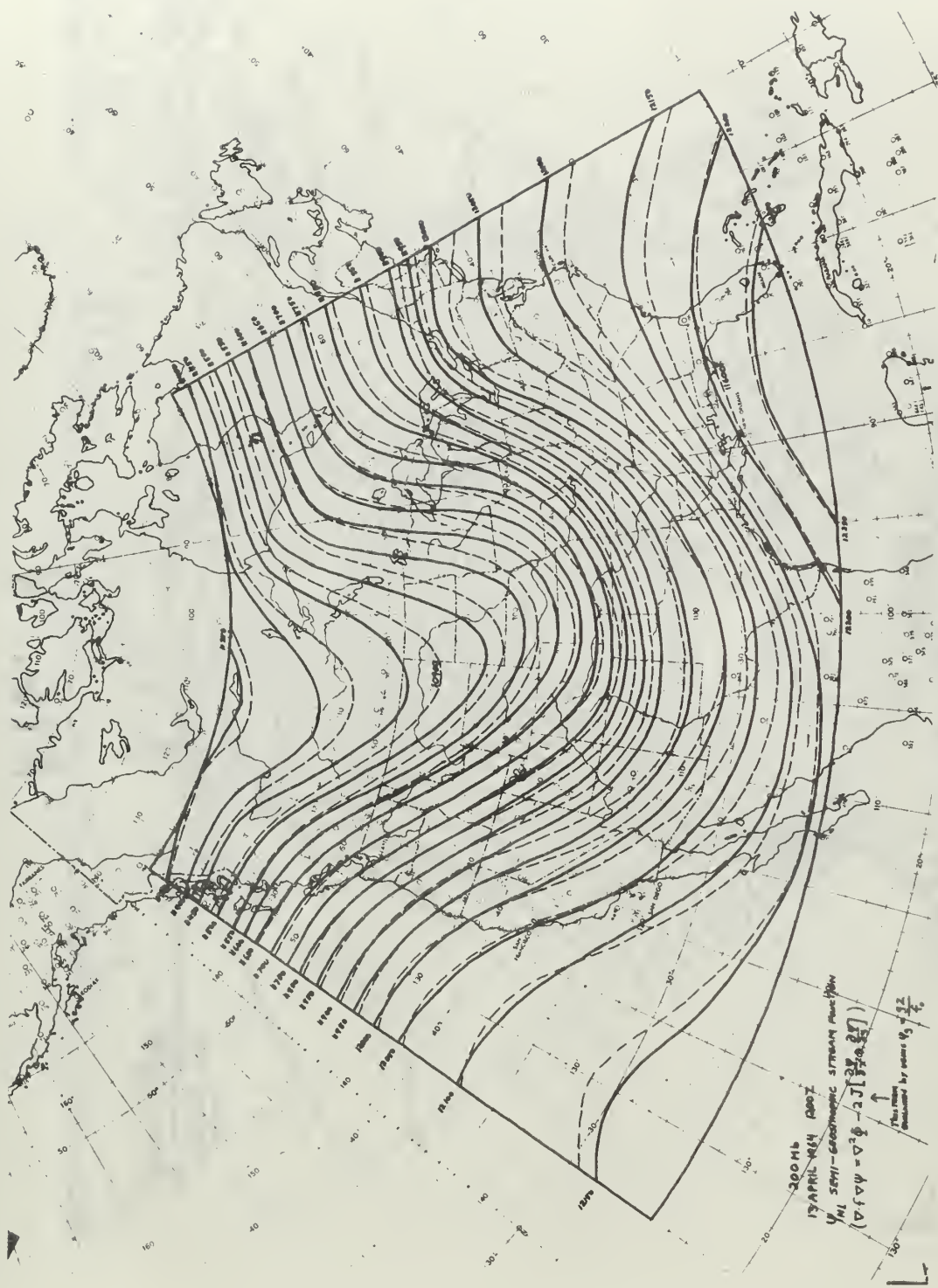


FIG. 3

200 mb
13 APRIL-MAY 1957
M1 5M11-GEOSTROPHIC STREAM FUNCTION
 $(\nabla^2 \psi = \sigma^2 \phi - \frac{1}{2} \nabla^2 (\frac{\partial \phi}{\partial t}))$
↑
This stream
function is
estimated by using $\phi_0 = \frac{1}{2} \frac{\partial \phi}{\partial t}$

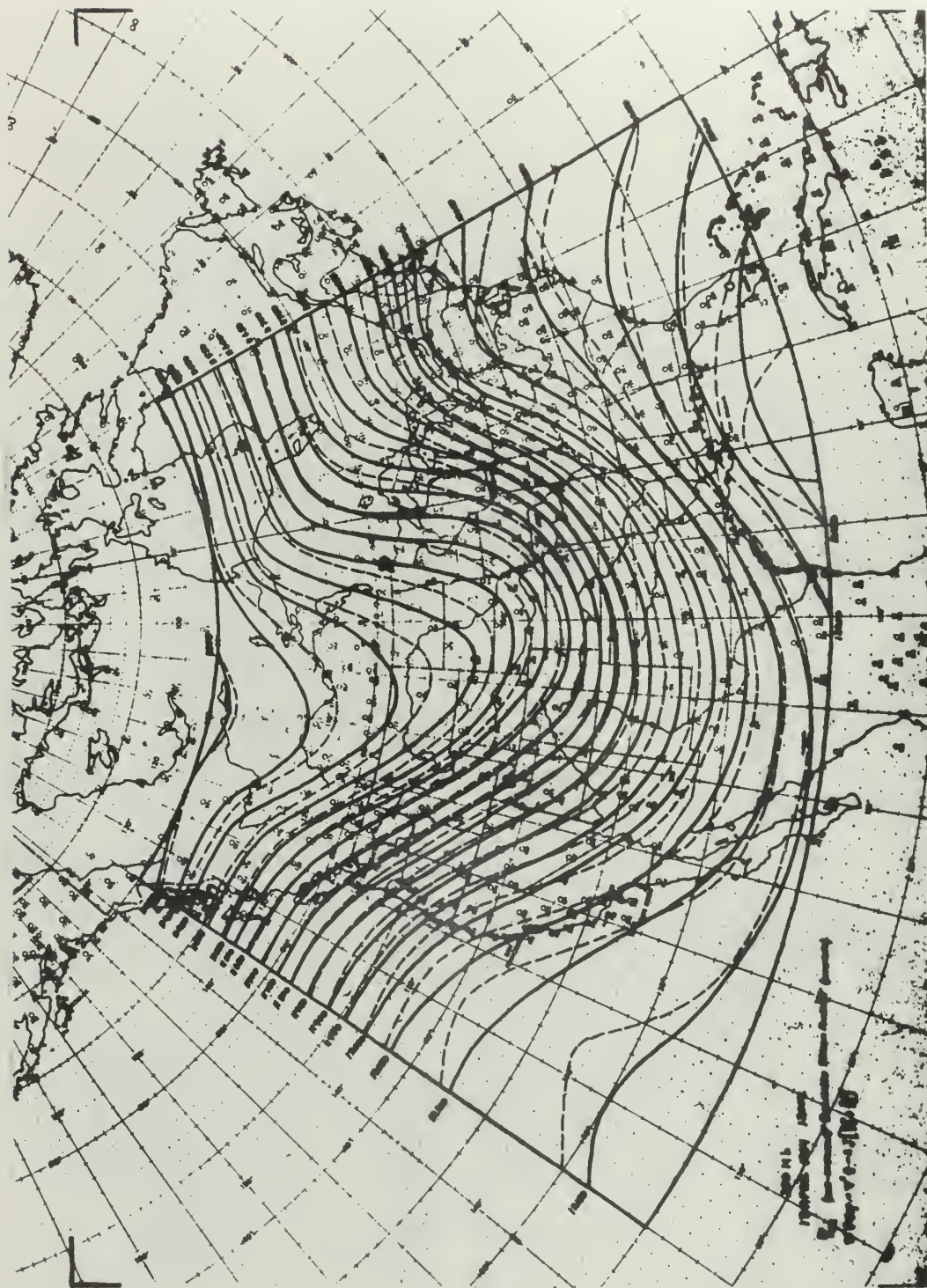


FIG. 4

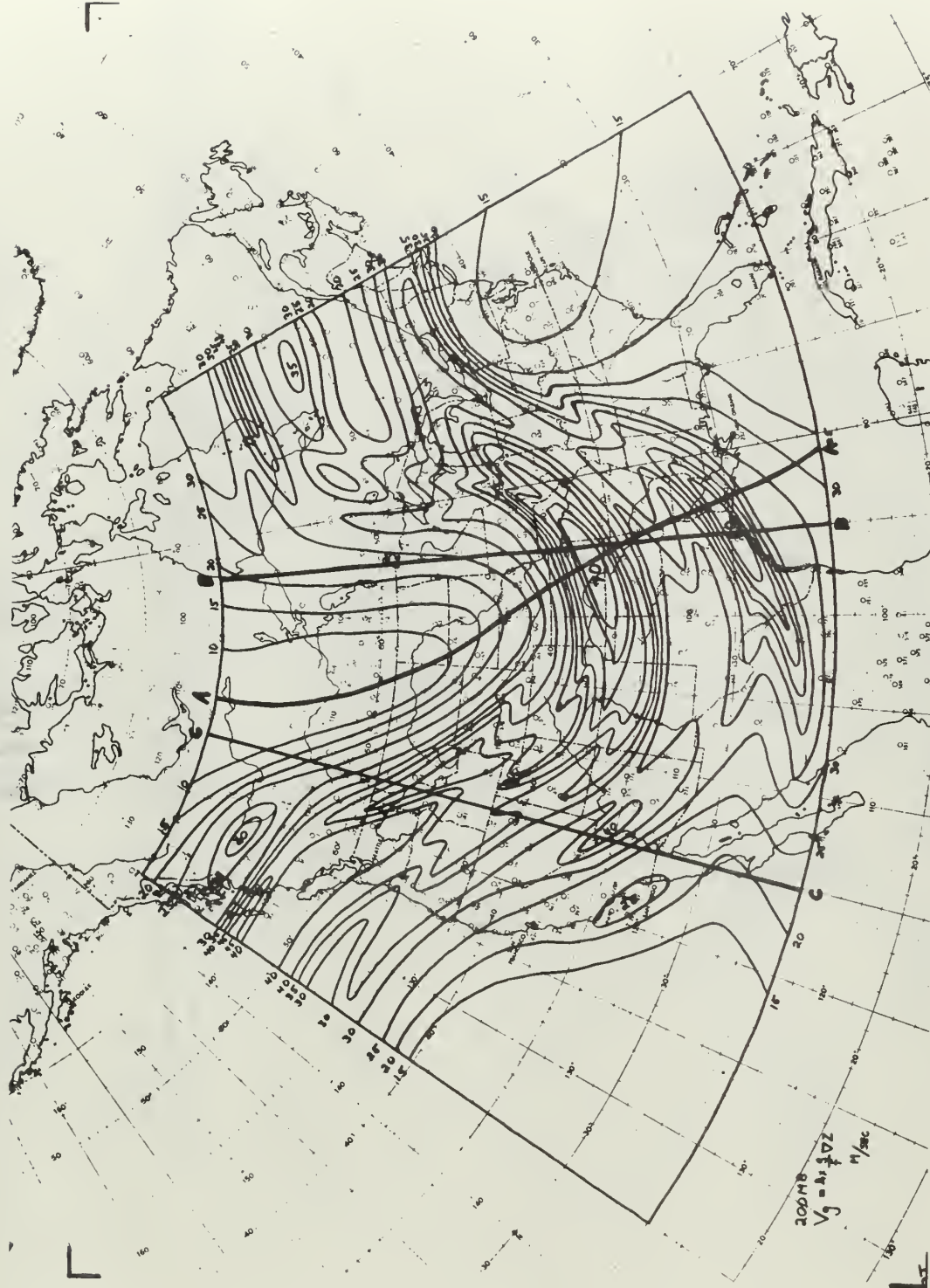


FIG. 5

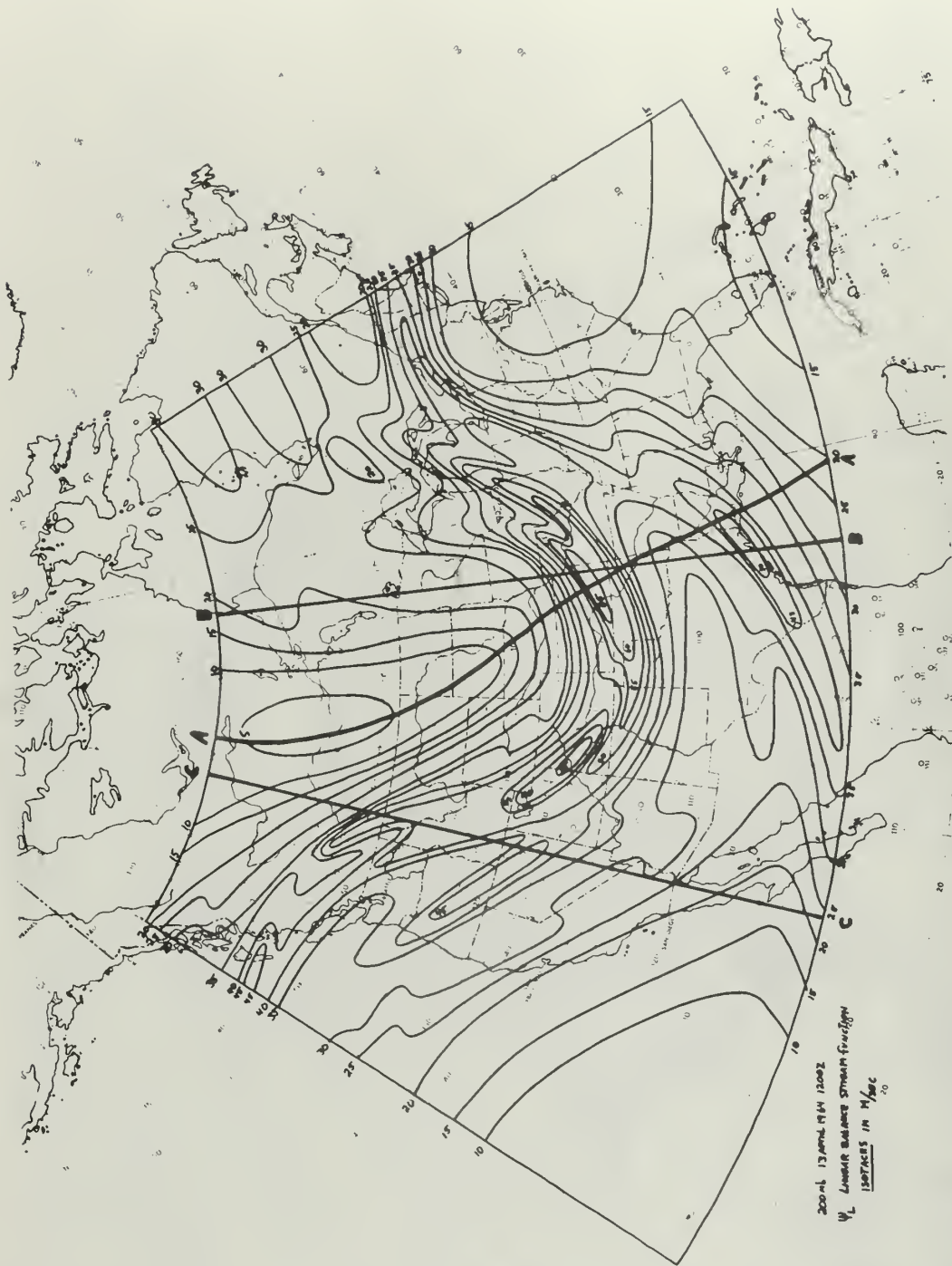


FIG. 6

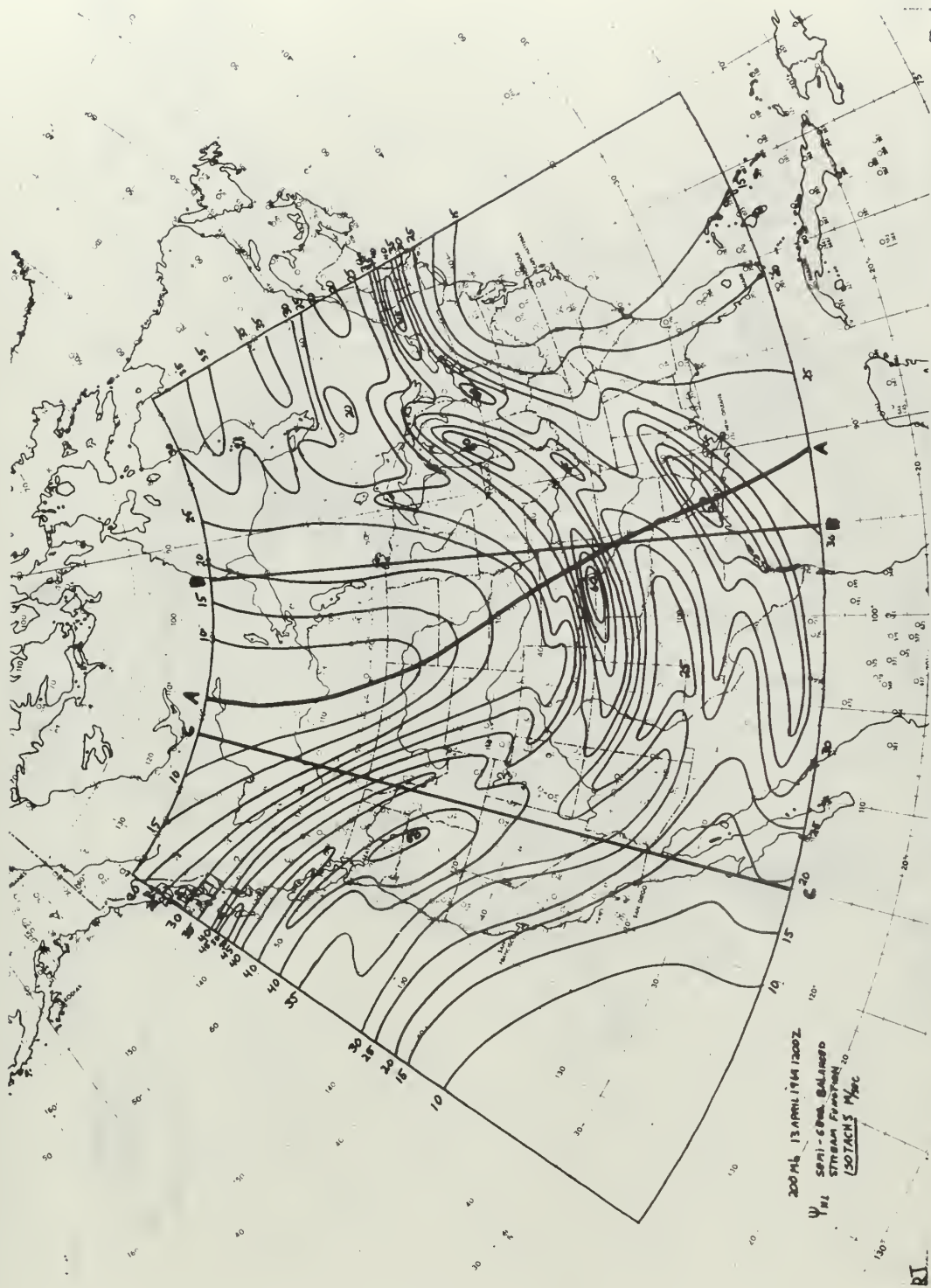


FIG. 7

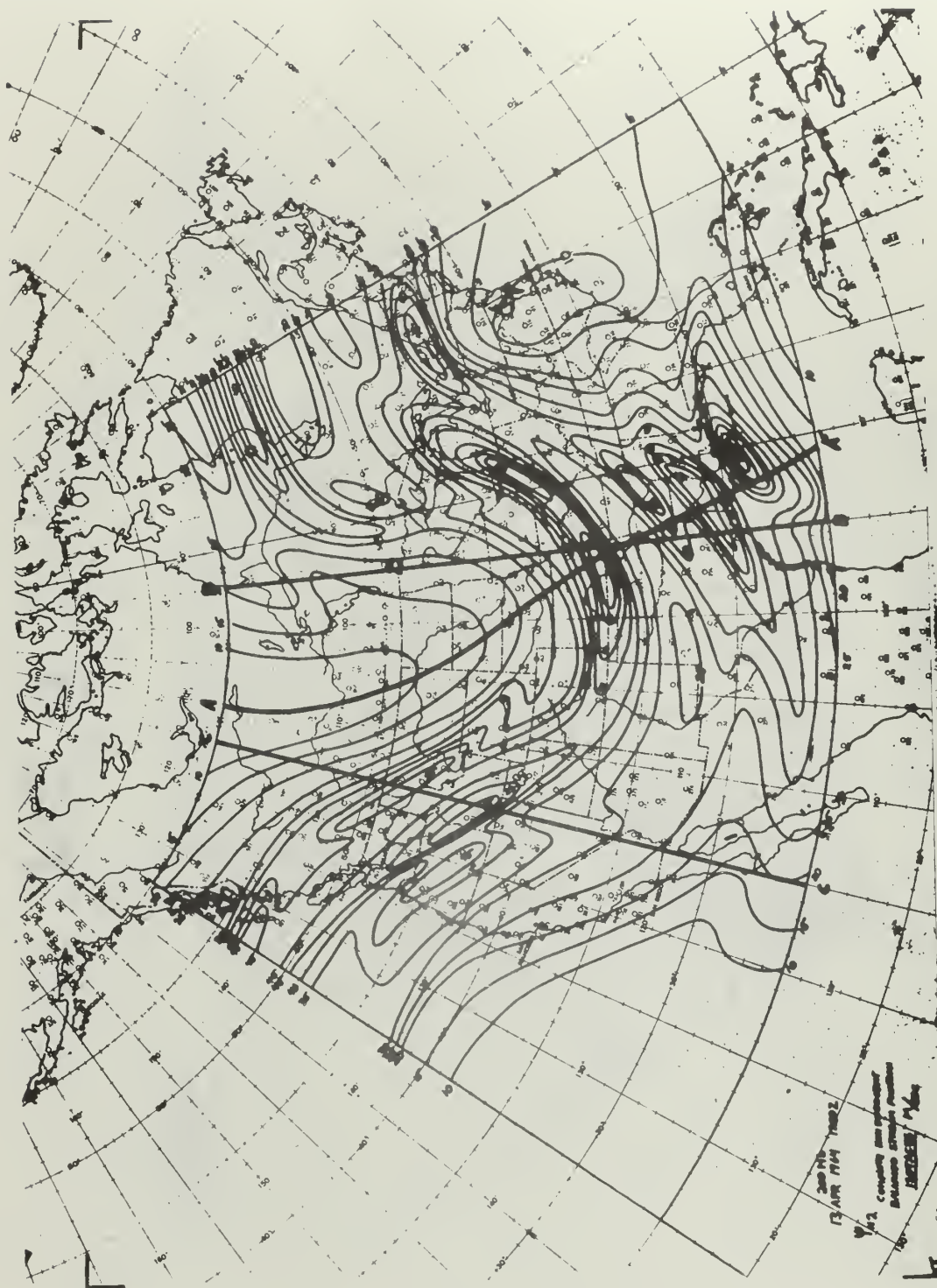
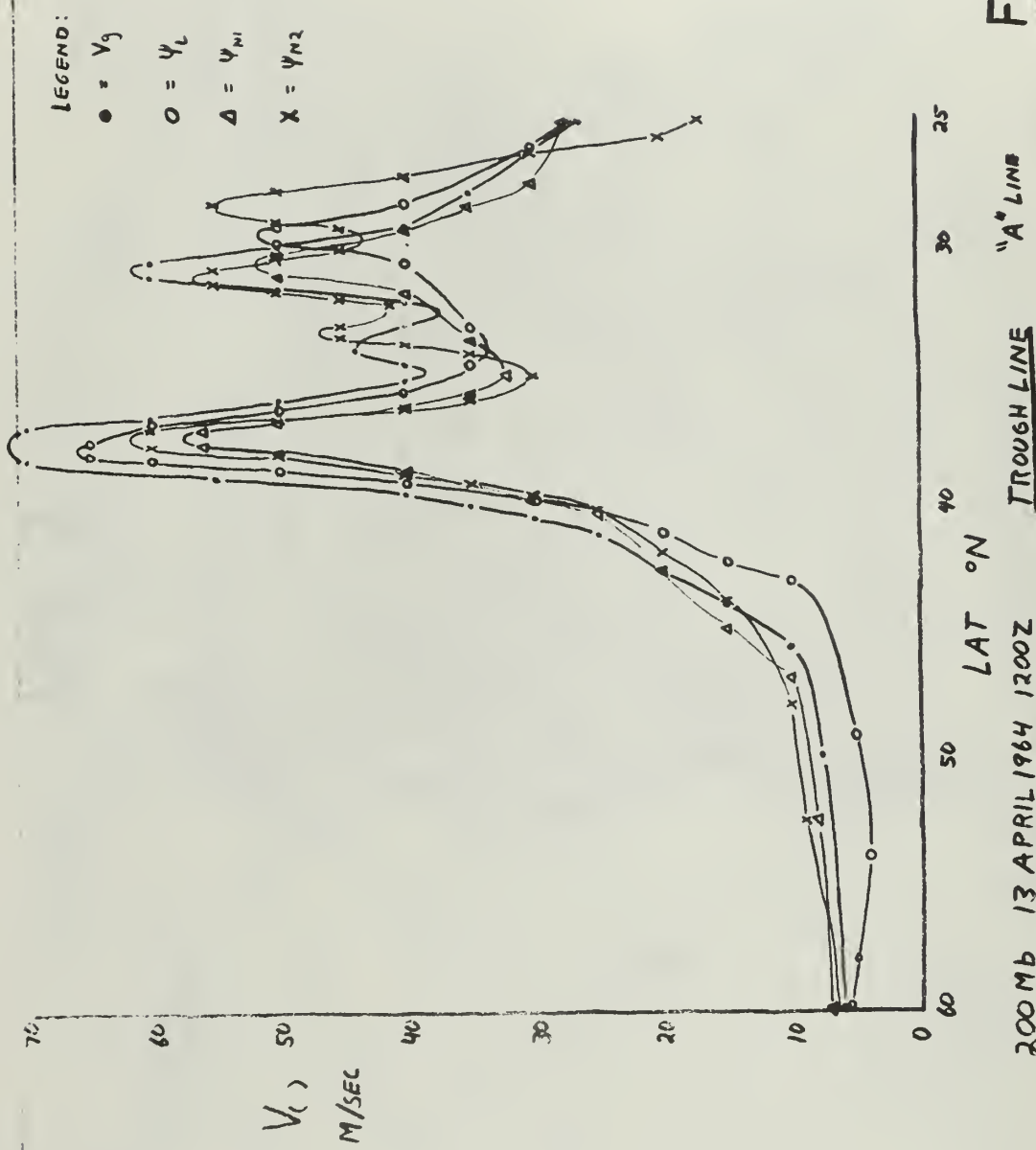


FIG. 8





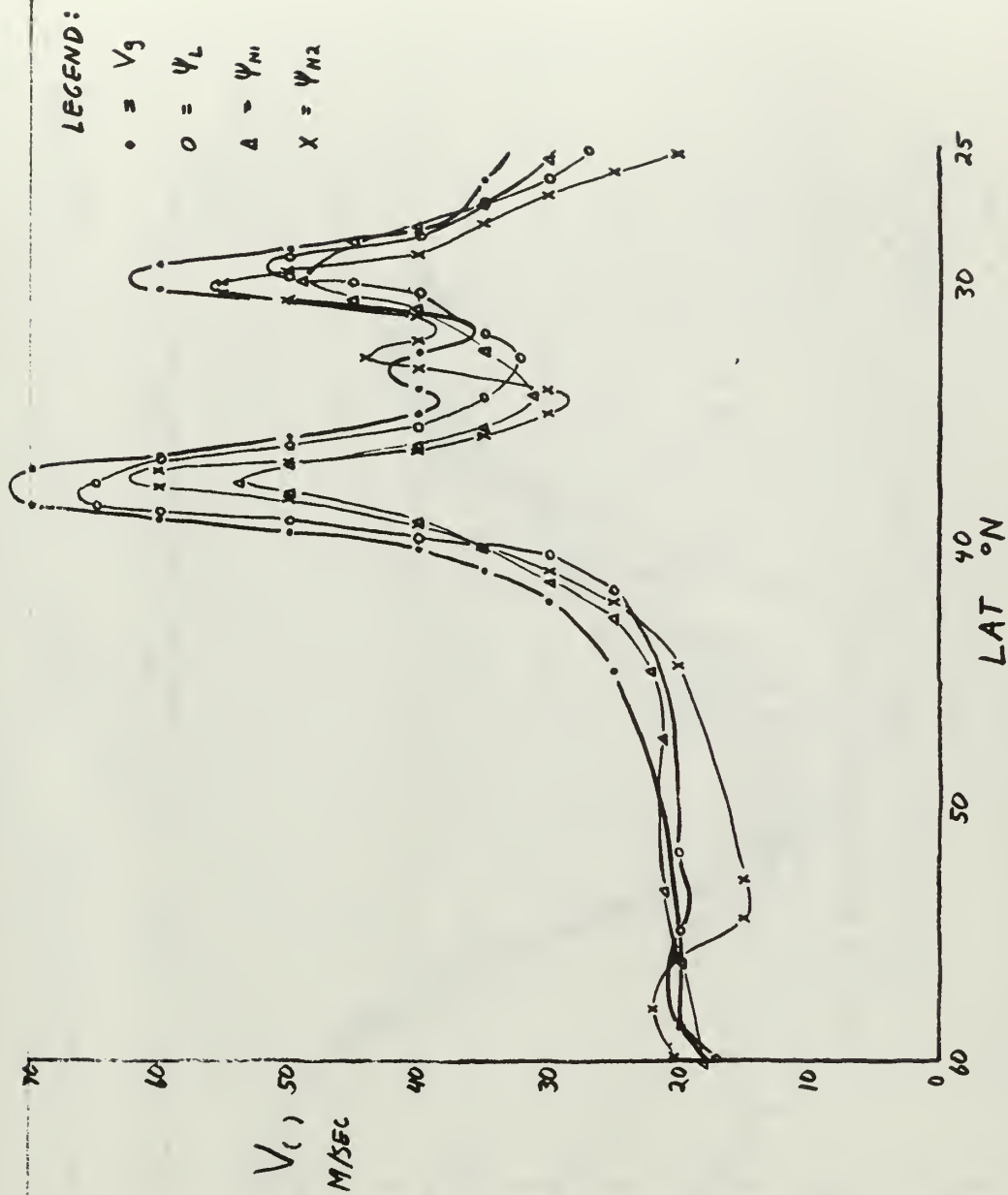
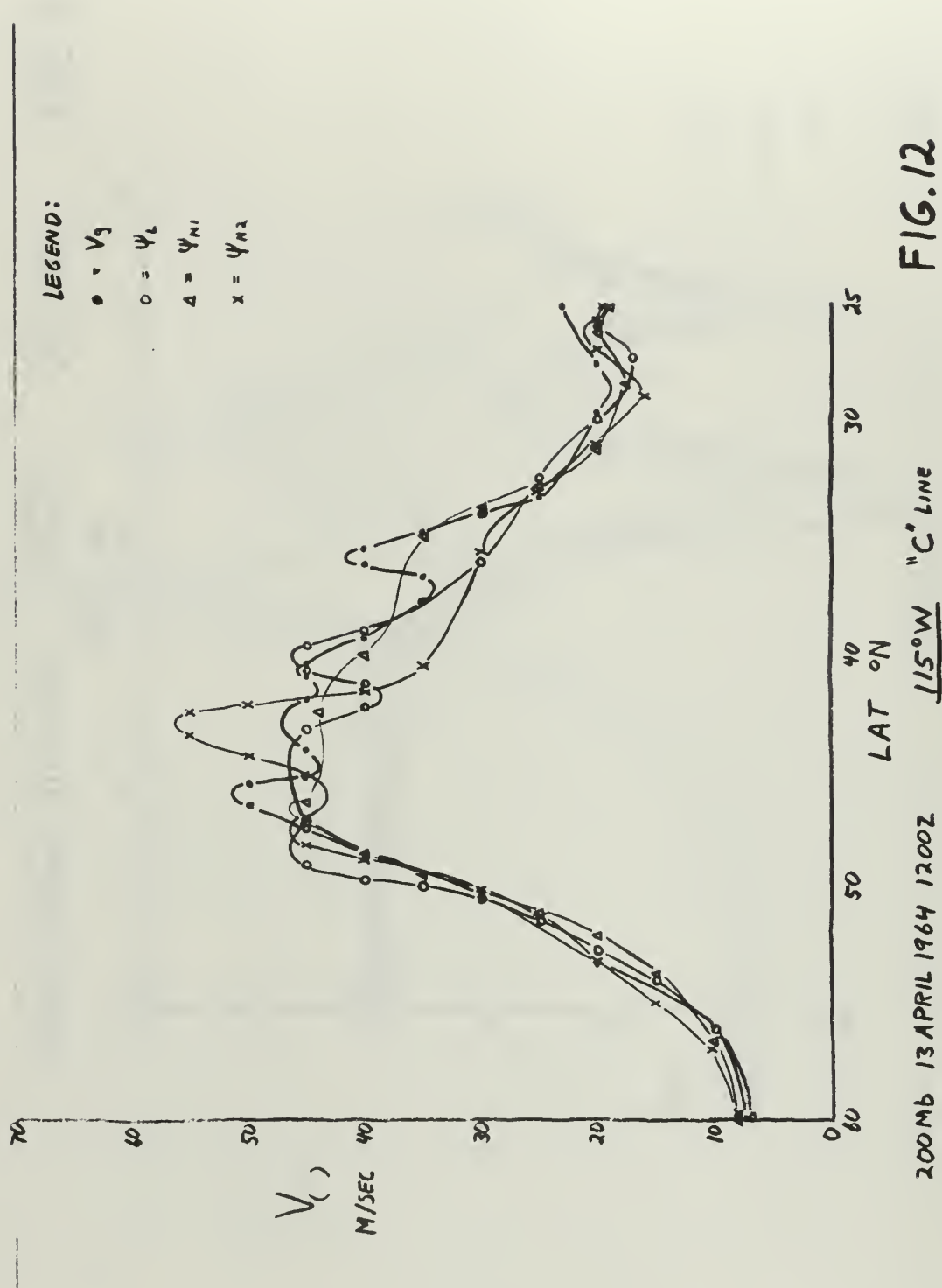


FIG. 11

"B" LINE

95°W

200 MB 13 APRIL 1964 1200Z



	No. $V_{(1)} - V_R$ > 0	No. $V_{(1)} - V_R$ < 0	No. $V_{(1)} - V_R$ > 10	No. $V_{(1)} - V_R$ < -10	AVG. $V_{(1)} - V_R$ POS.	AVG. $V_{(1)} - V_R$ NEG.	OVERALL MEAN DIFFERENCE
V_G	43	25	31	13	10.4	5.7	+ 4.51
V_{ψ_L}	45	23	22	15	5.7	7.9	+ 1.06
$V_{\psi_{H1}}$	42	26	22	16	5.6	8.6	+ 0.18
$V_{\psi_{H2}}$	37	31	22	18	5.3	9.0	+ 1.22

OF 68 REPORTED WINDS:
 $V_{(1)} - V_R$ = POS IF 0 OR +
 = NEG IF —

FIG. 13

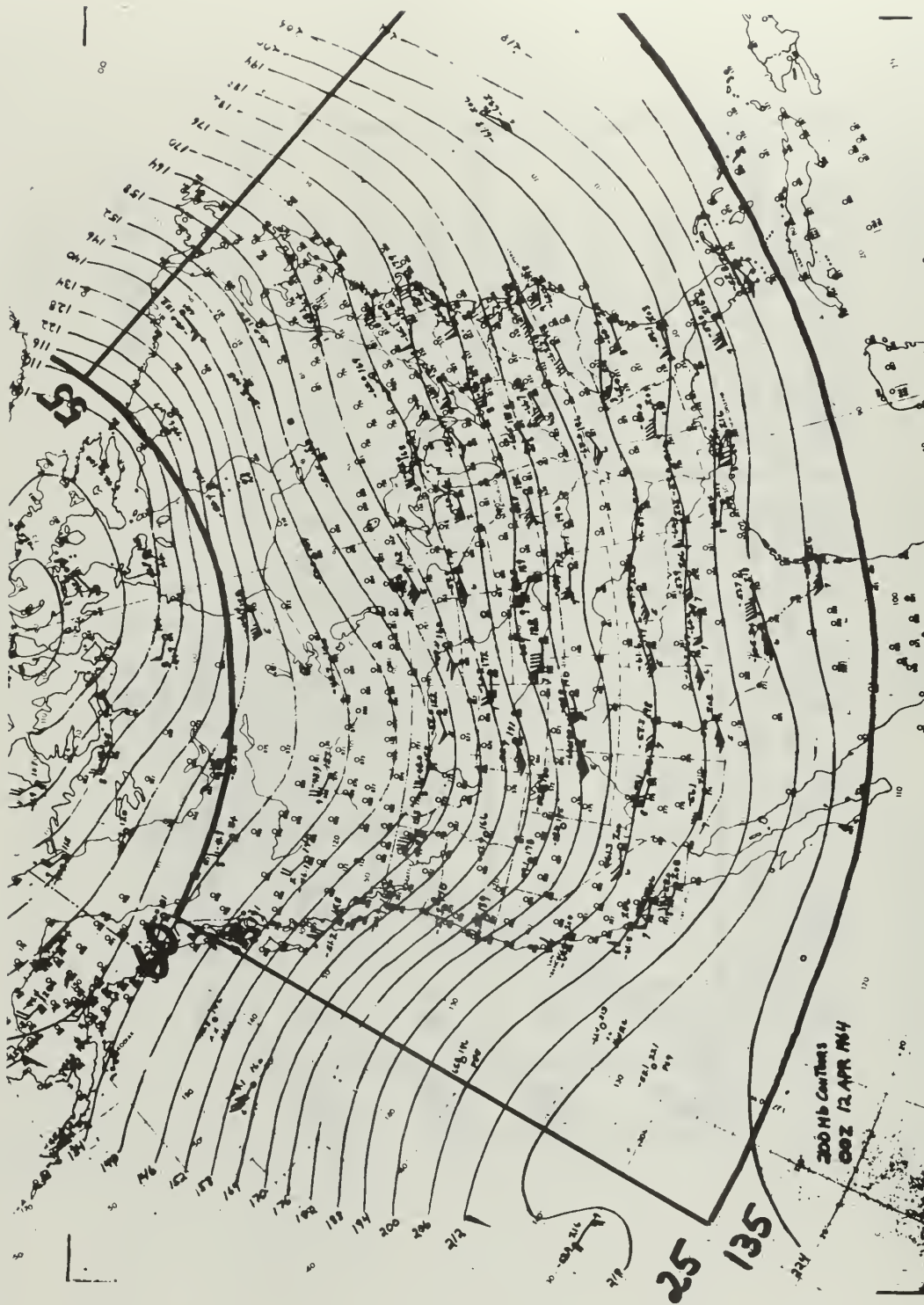
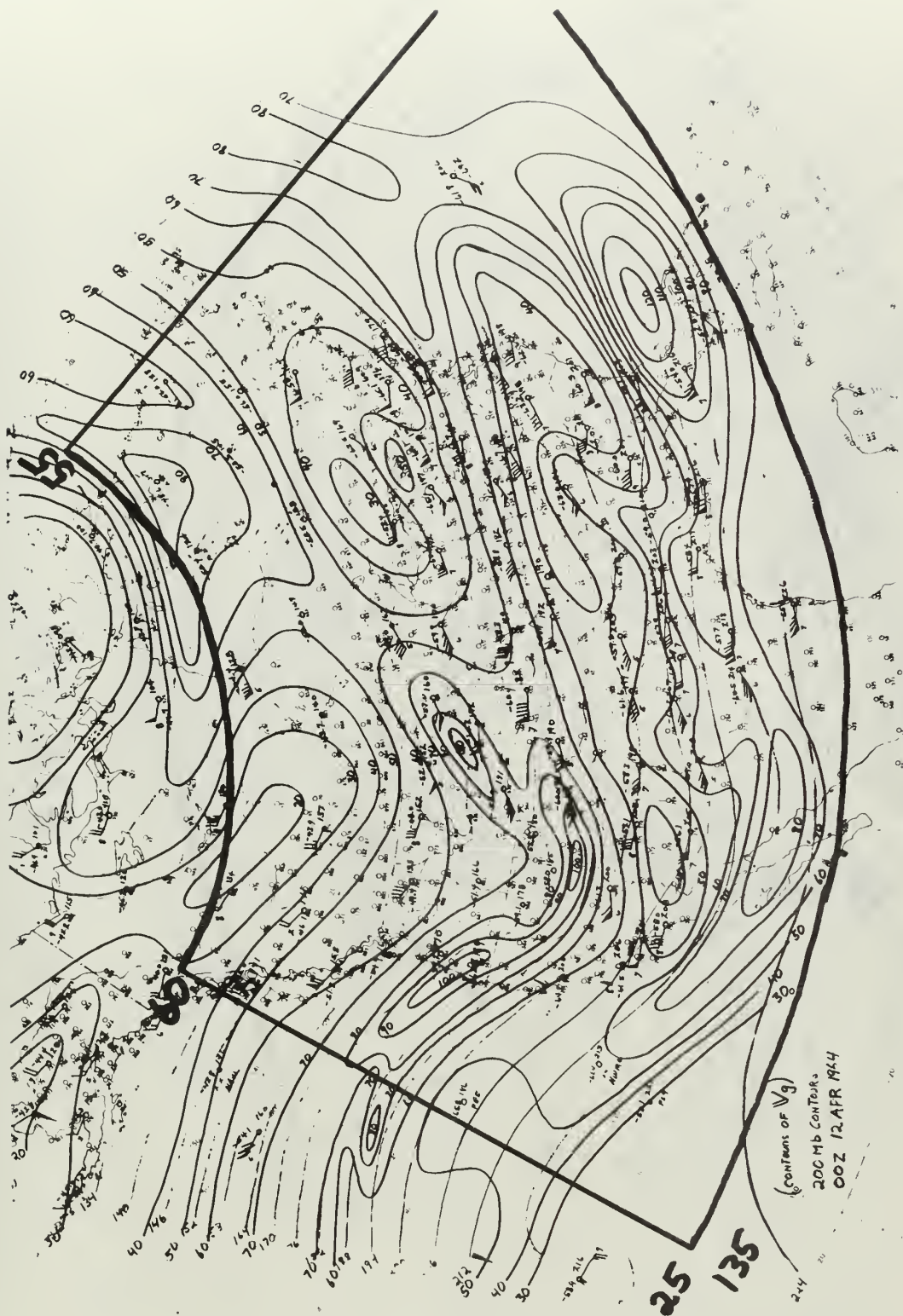


FIG. 14



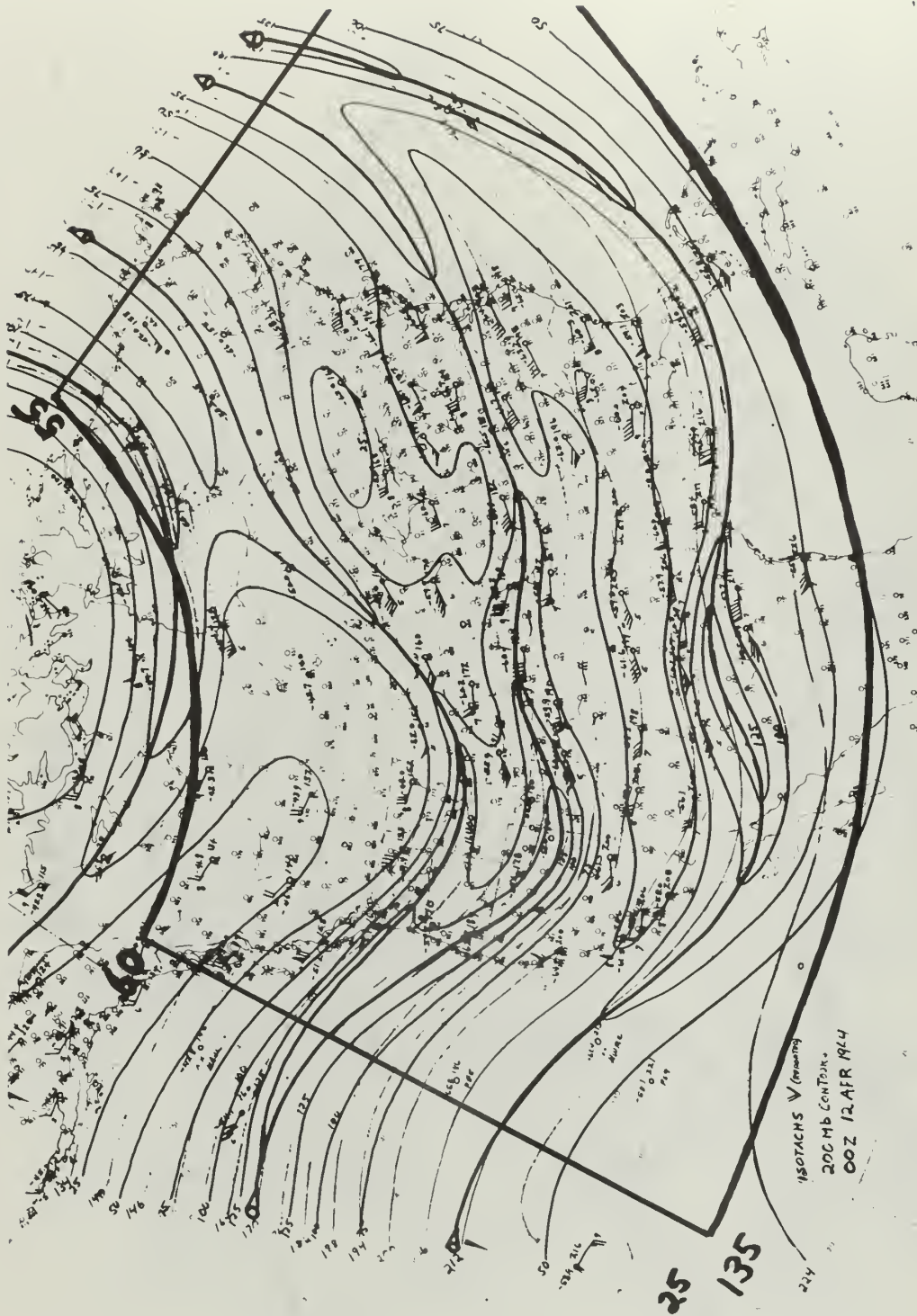


FIG. 16

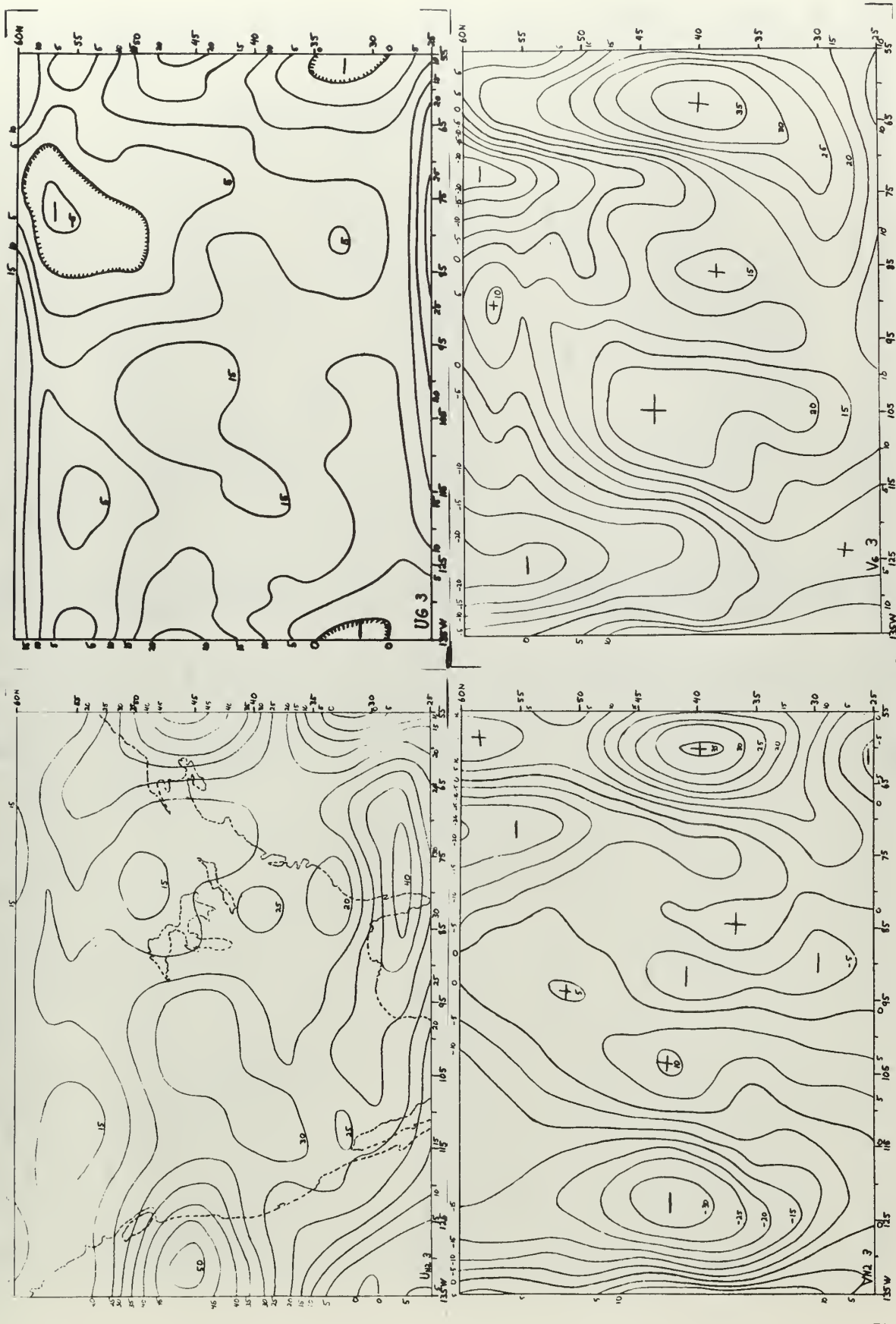


FIG. 17

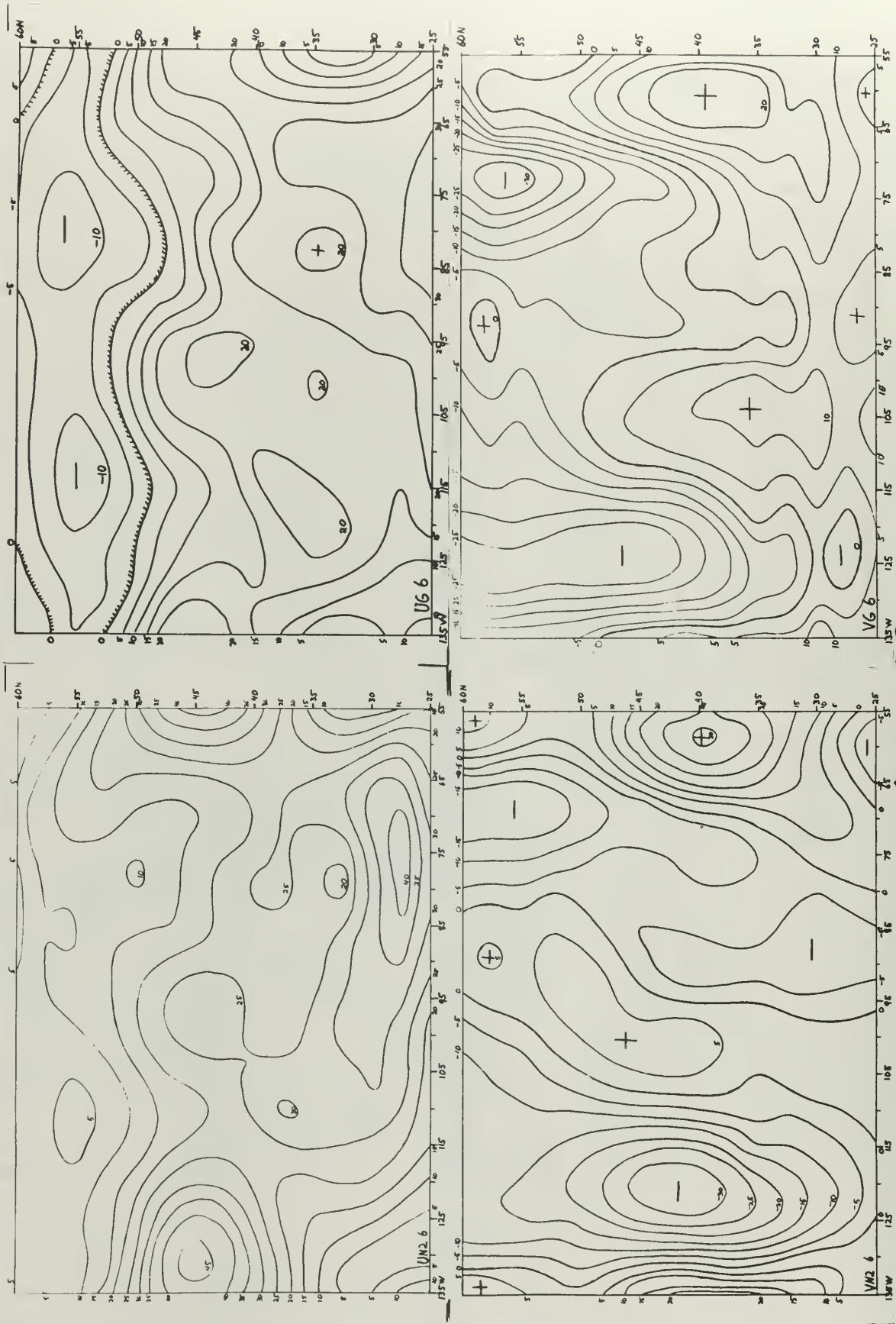


FIG. 18

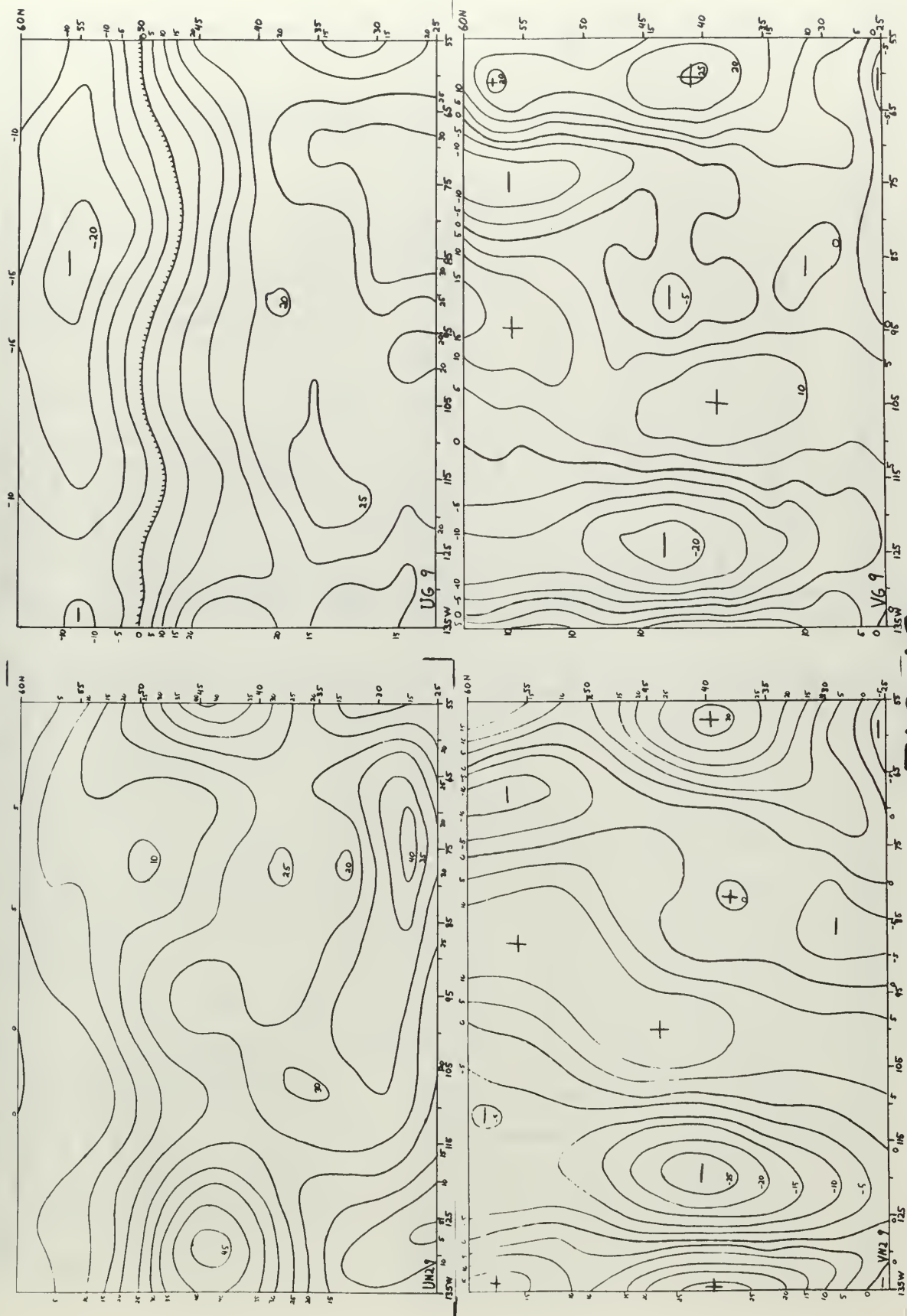


FIG. 19

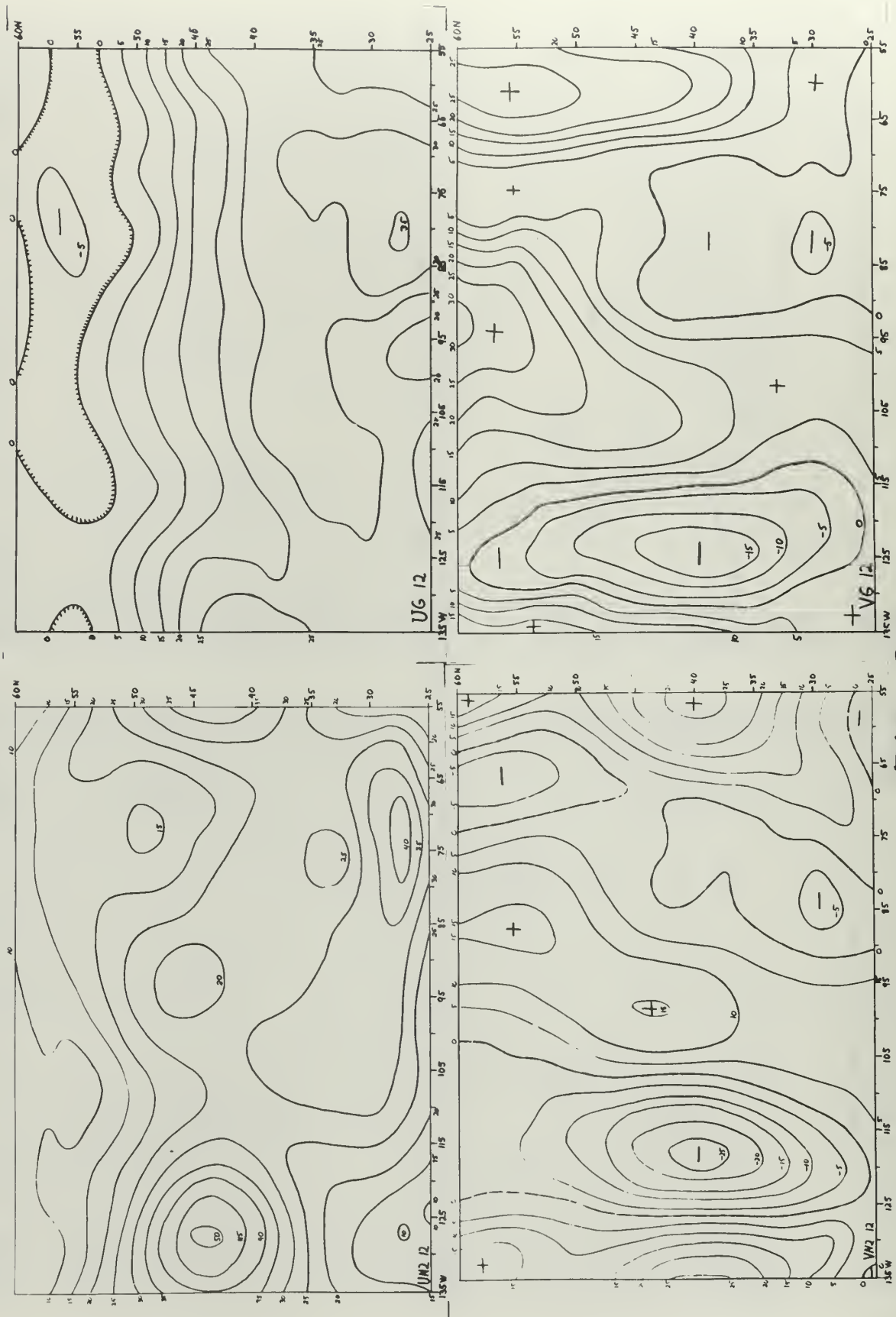


FIG. 20

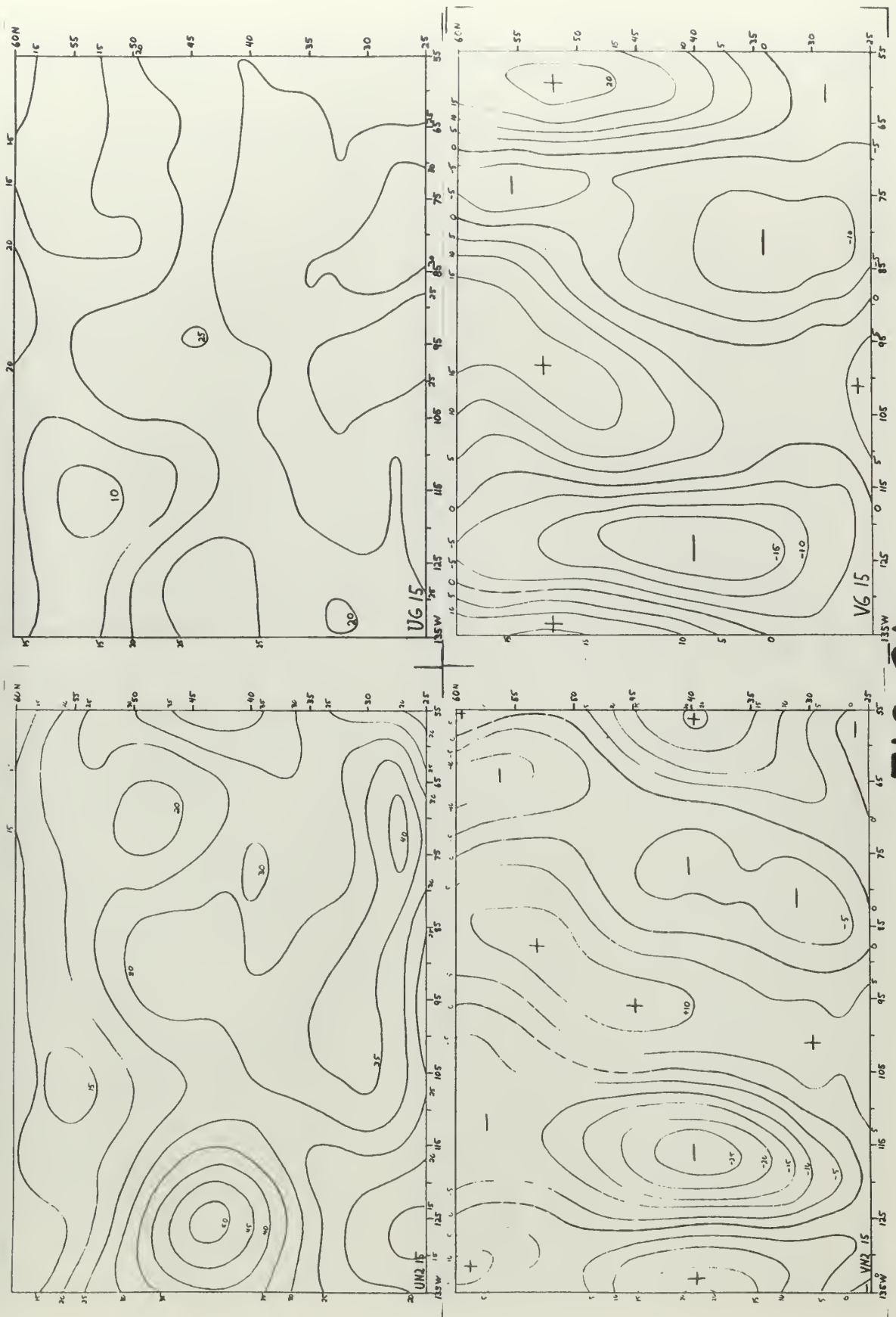


FIG. 21

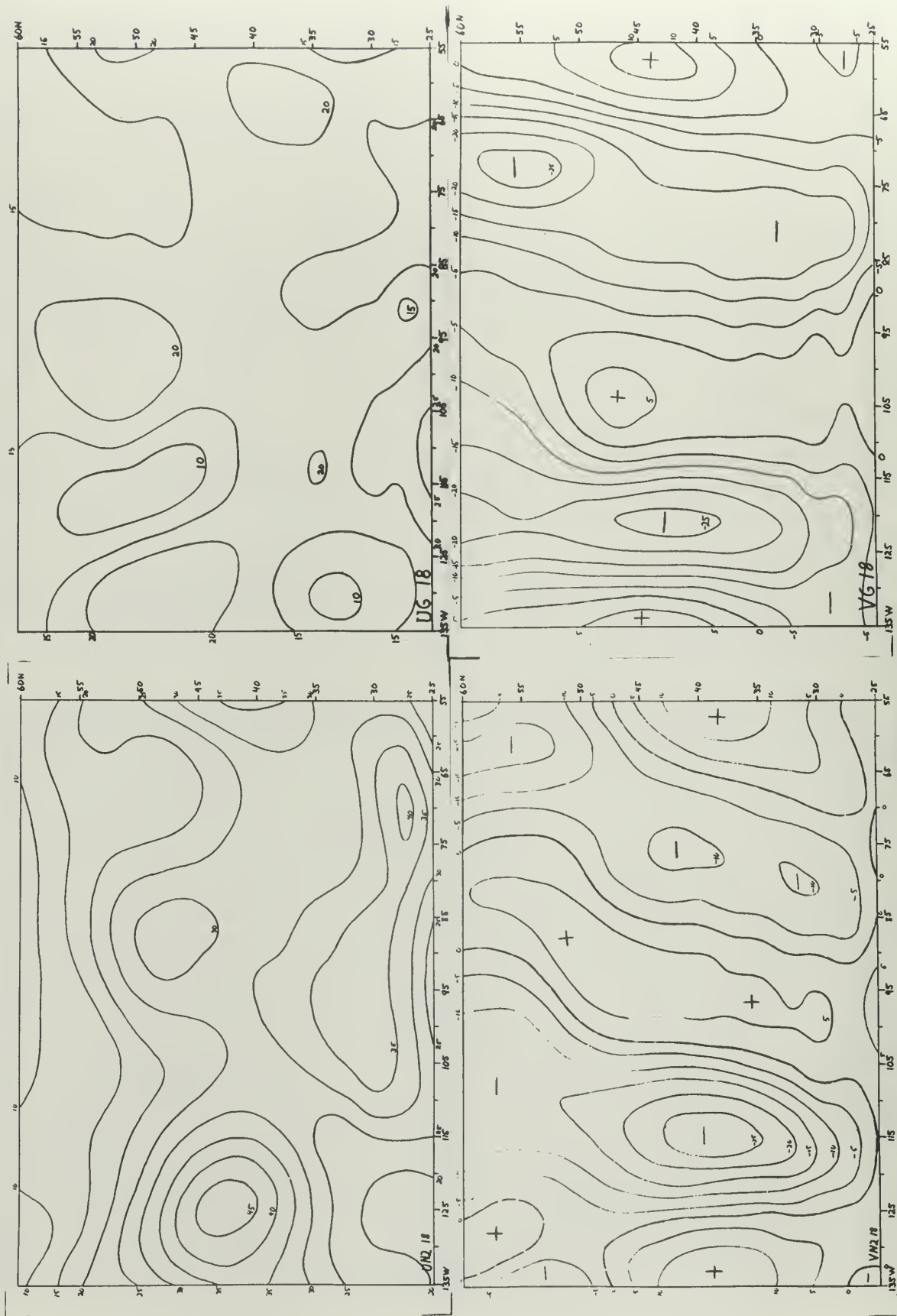


FIG. 22

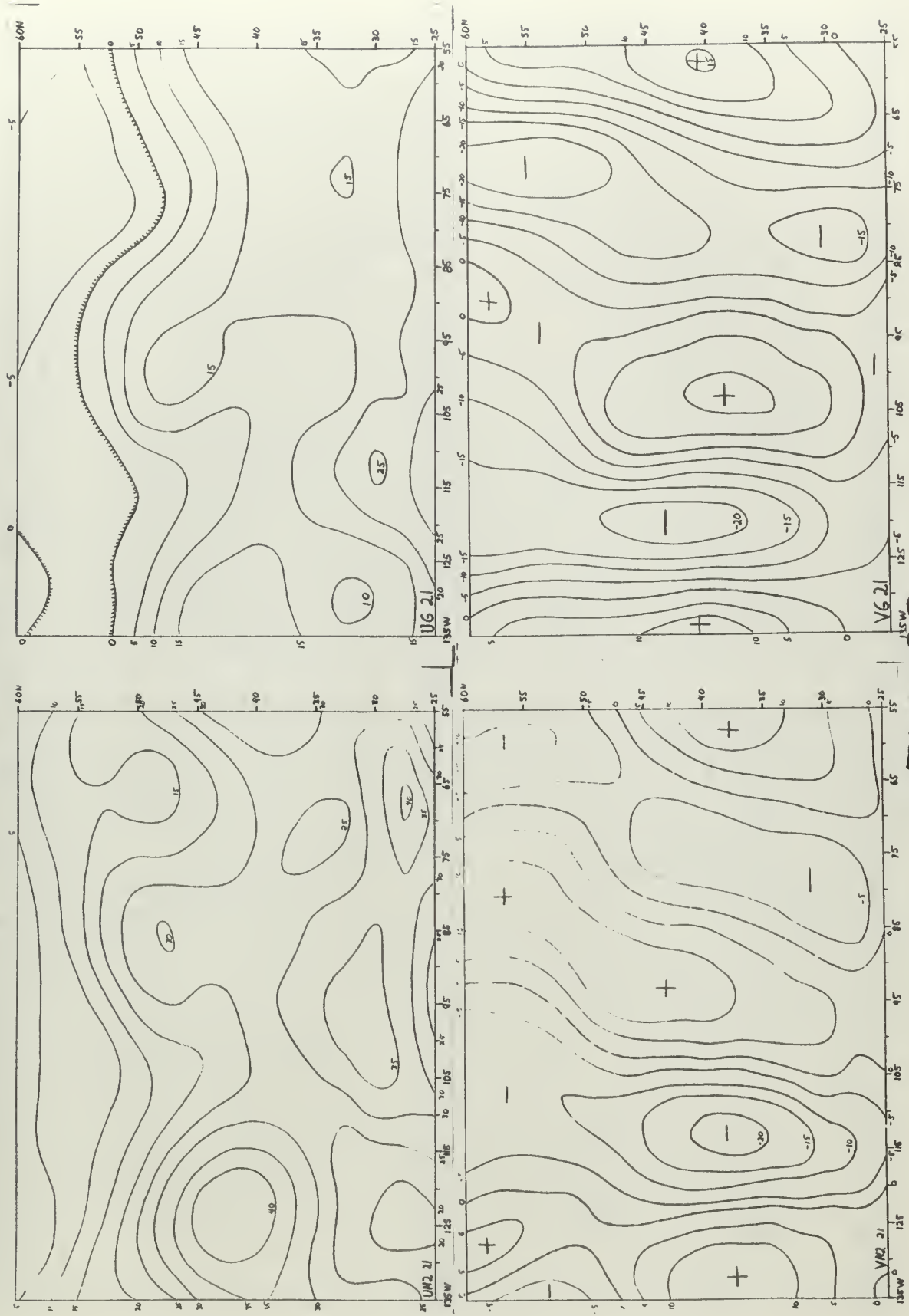


FIG. 23

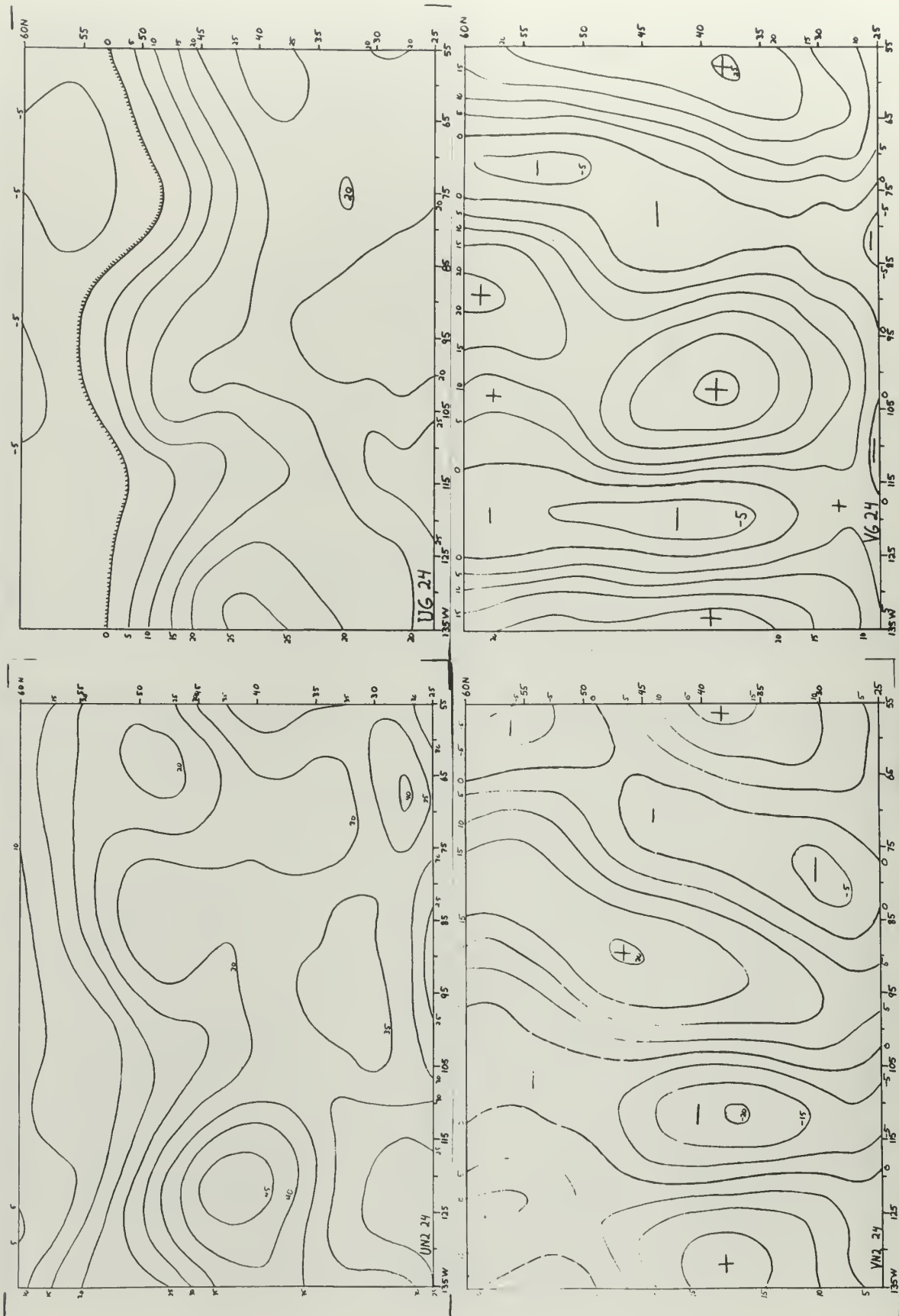


FIG. 24

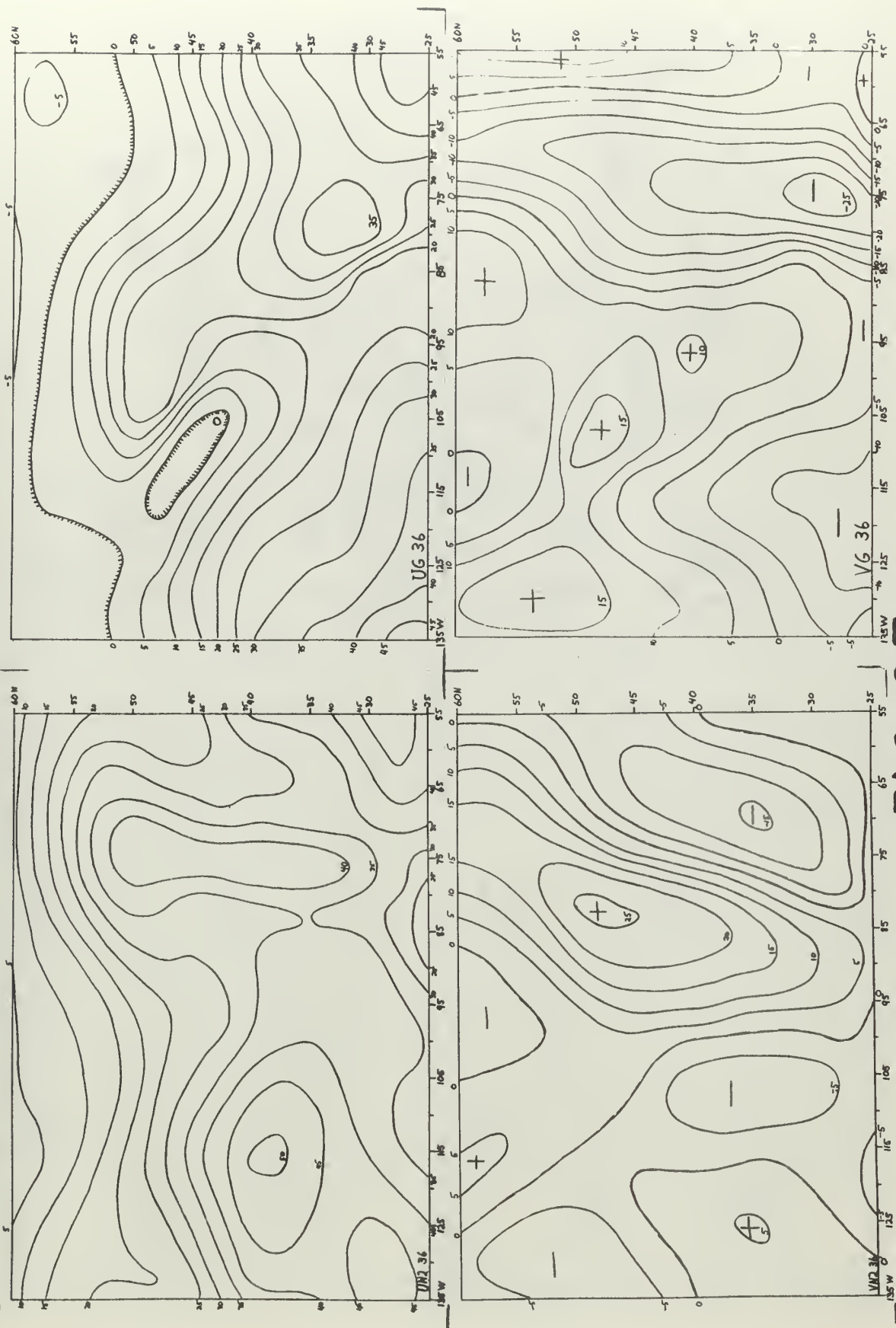


FIG. 25

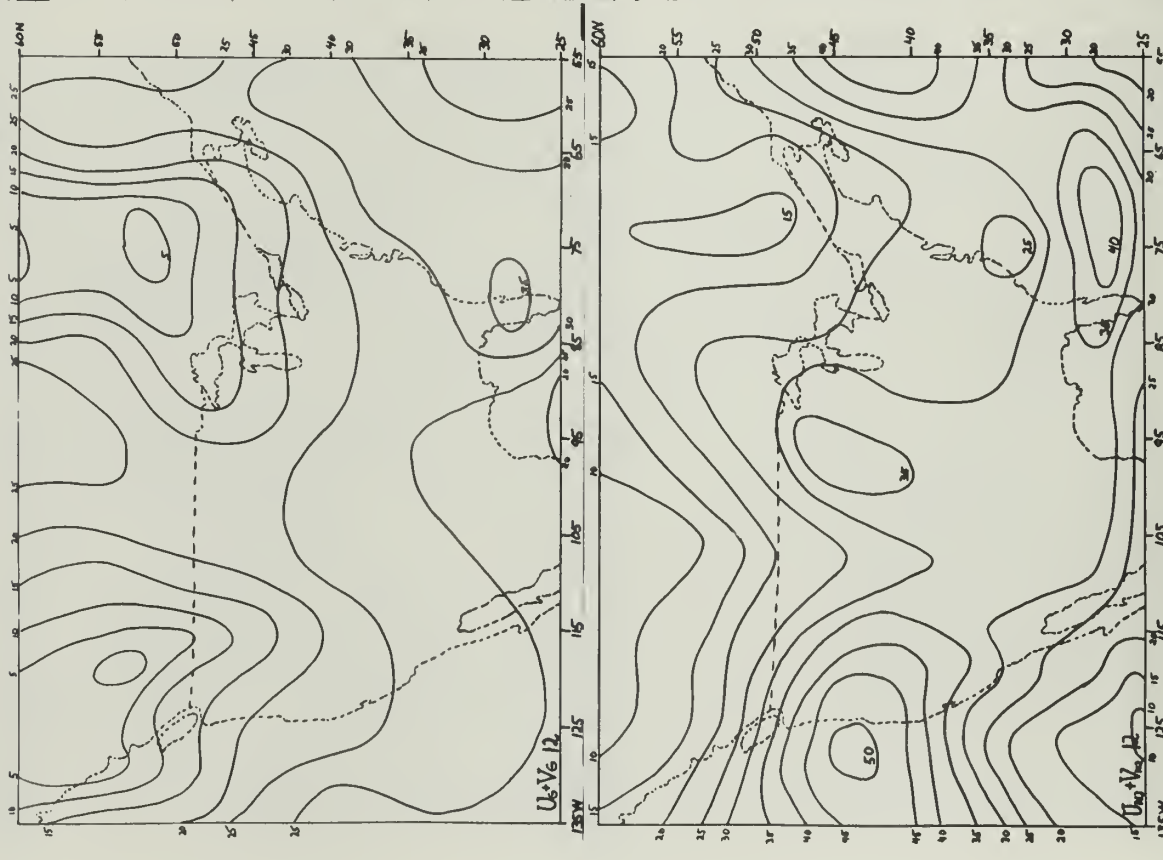
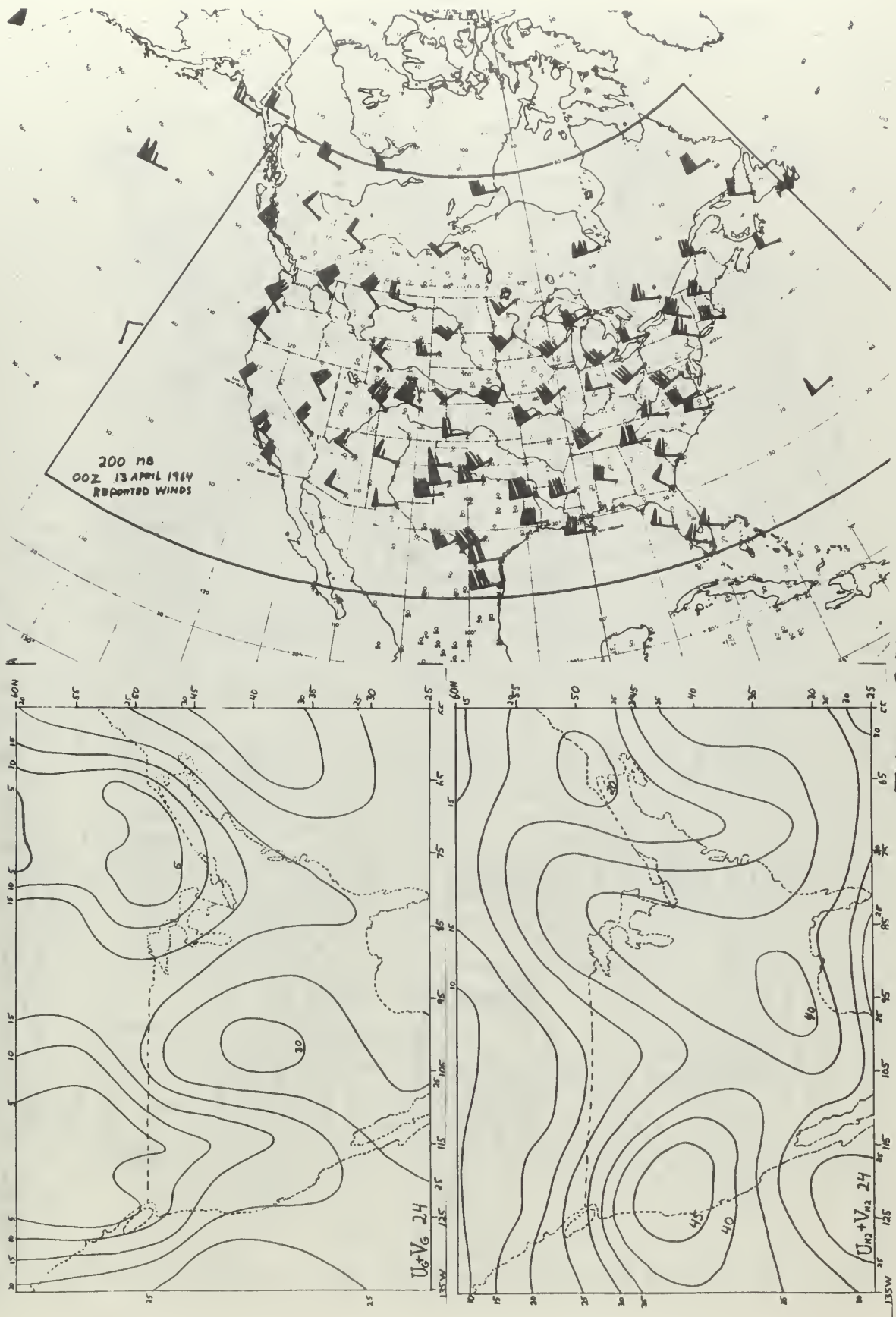


FIG. 26



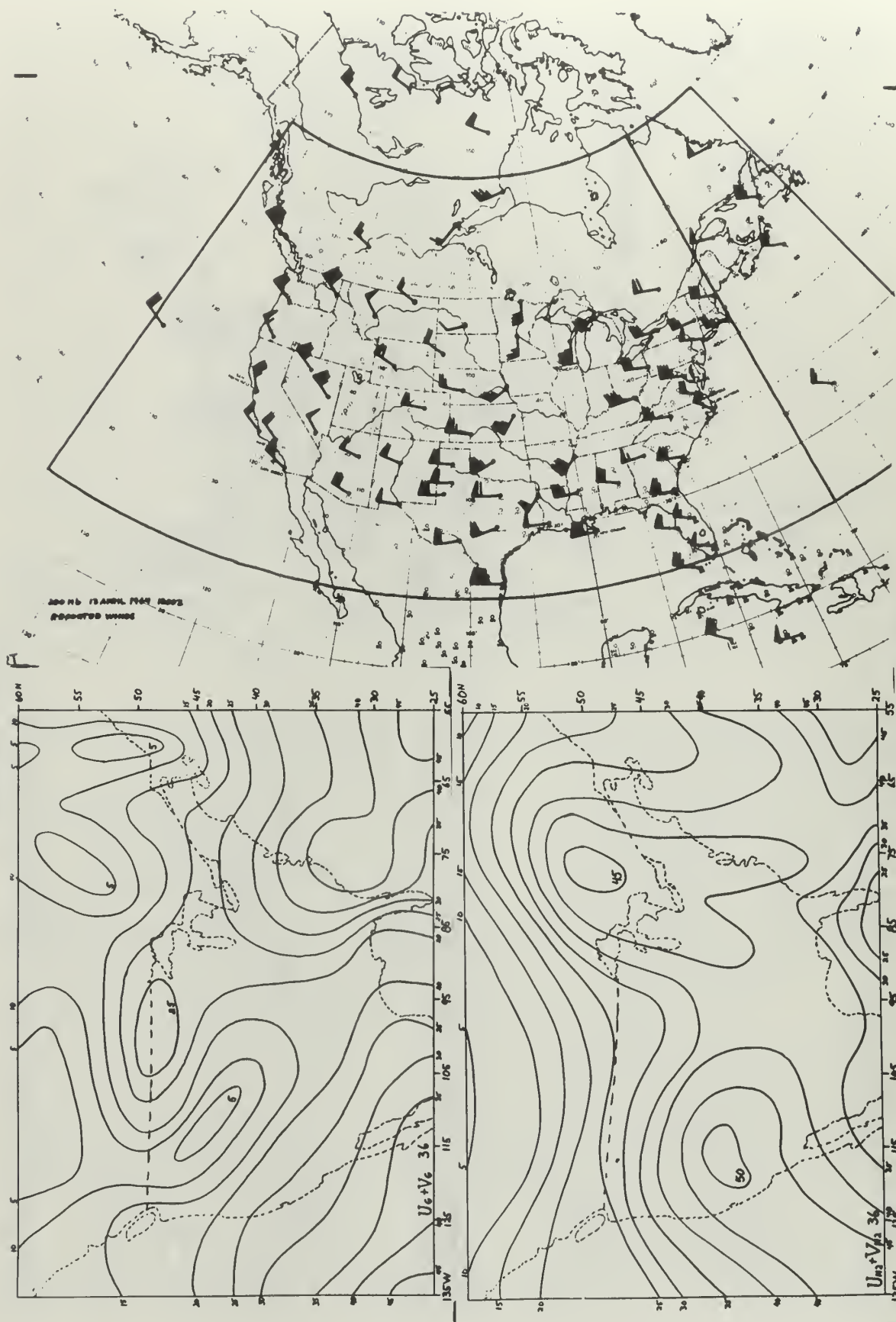


FIG. 28

	# V_R COMPARED		$V_{(1)} - V_R$, # < -10MT	$V_{(1)} - V_R$, # > 10MT	AVG. NEG. ERROR	AVG. POS. ERROR	MEAN ERROR
12 hr	NEG	POS					
$V_g - V_R$	48	30	28	20	-10.6	+4.8	-4.5
25-40	26	15	15	12	-9.9	+7.1	-3.7
40-60	22	15	13	8	-11.4	+3.4	-5.4
$V_{N2} - V_R$	28	50	11	22	-3.8	+5.1	+1.9
25-40	17	25	8	13	-4.5	+5.8	+1.6
40-60	12	25	3	9	-3.3	+4.4	+2.0
24 hr							
$V_g - V_R$	53	20	43	7	-16.9	+4.3	-9.8
25-40	28	12	22	1	-13.1	+0.5	-9.0
40-60	25	8	21	6	-21.1	+10.0	-13.7
$V_{N2} - V_R$	17	56	10	31	-5.7	+5.9	+3.2
25-40	6	32	2	19	-1.2	+6.7	+5.4
40-60	11	24	8	12	-8.1	+4.9	+0.86
36 hr							
$V_g - V_R$	36	31	30	19	-19.4	+9.6	-6.0
25-40	22	19	16	15	-17.2	+14.2	-2.6
40-60	14	12	14	4	-24.6	+2.5	-12.1
$V_{N2} - V_R$	9	58	6	44	-8.3	+17.2	+13.9
25-40	4	35	2	26	-7.2	+18.9	+16.3
40-60	5	23	4	18	-9.2	+14.7	+10.4
	g = QUASI-GEOSTROPHIC R = REPORTED N2 = COMPLETE BALANCED $V_{(1)} - V_R$ = POS IF + or 0 = NEG IF -					FIG. 29	

INITIAL DISTRIBUTION LIST

	<u>No. Copies</u>
1. LT R. B. Brodehl, USN Naval Weather Facility Naval Air Station Norfolk, Virginia 23511	3
2. Prof T. N. Krishnamurti (Thesis Advisor) Department of Meteorology Florida State University Tallahassee, Florida 32306	2
3. Library Naval Postgraduate School Monterey, California 93940	2
4. Dept. of Meteorology & Oceanography Naval Postgraduate School Monterey, California 93940	3
5. R. J. Renard Dept. of Meteorology & Oceanography Naval Postgraduate School Monterey, California 93940	1
6. Defense Documentation Center Cameron Station Alexandria, Virginia 22314	20
7. Naval Weather Service Command Naval Station (Washington Navy Yard Annex) Washington, D. C. 20390	1
8. Officer in Charge Naval Weather Research Facility Naval Air Station, Building R-48 Norfolk, Virginia 23511	2
9. Officer in Charge Fleet Numerical Weather Facility Naval Postgraduate School Monterey, California 93940	1

		<u>No. Copies</u>
10.	Director, Naval Research Laboratory ATTN: Tech. Services Information Officer Washington, D. C. 20390	1
11.	AFCRL - Research Library L. G. Hanscom Field ATTN: Nancy Davis/Stop 29 Bedford, Massachusetts 01730	
12.	Program Director for Meteorology National Science Foundation Washington, D. C. 20550	1
13.	Commander, Air Weather Service Military Airlift Command U. S. Air Force Scott Air Force Base, Illinois 62226	2
14.	Office of Naval Research Department of the Navy Washington, D. C. 20360	1
15.	Department of Commerce, ESSA Weather Bureau Washington, D. C. 20235	2

Security Classification

DOCUMENT CONTROL DATA - R&D

(Security classification of title, body of abstract and indexing annotation must be entered when the overall report is classified)

1. ORIGINATING ACTIVITY (Corporate author) Naval Postgraduate School Monterey, California 93940		2a. REPORT SECURITY CLASSIFICATION UNCLASSIFIED	
		2b. GROUP	
3. REPORT TITLE A COMPARISON OF FOUR NON-DIVERGENT WIND FIELDS			
4. DESCRIPTIVE NOTES (Type of report and inclusive dates) Master of Science Thesis in Meteorology			
5. AUTHOR(S) (Last name, first name, initial) BRODEHL, Richard Brian, Lieutenant, USN			
6. REPORT DATE September 1967	7a. TOTAL NO. OF PAGES 55	7b. NO. OF REFS 9	
8a. CONTRACT OR GRANT NO.	9a. ORIGINATOR'S REPORT NUMBER(S)		
b. PROJECT NO.			
c.	9b. OTHER REPORT NO(S) (Any other numbers that may be assigned this report)		
d.			
10. AVAILABILITY/LIMITATION NOTICES This report is subject to special export control and is not to be distributed outside the United States without prior approval of the Department of Defense.			
11. SUPPLEMENTARY NOTES		12. SPONSORING MILITARY ACTIVITY	
13. ABSTRACT <p>This paper is concerned with the comparison of four different non-divergent wind fields obtained from a single geopotential height field over a dense data area. After developing the divergence equation of the non-divergent stream function, four different stream functions are obtained by modification and/or deletion from the basic equation. Isotach patterns for each stream function are computed. A comparison of the four stream function patterns and their corresponding isotach patterns is made. Two of the stream functions are used to obtain the non-divergent wind field for the initial wind conditions in a primitive equation model developed by Krishnamurti. Two 36-hour forecasts are made. A comparison of the forecasts is made at three-hour intervals up to 24 hours and at 36 hours. Both forecasts are compared to the reported winds at 12-hour intervals.</p>			

KEY WORDS

LINK A

LINK B

LINK C

ROLE

WT

ROLE

WT

ROLE

WT

BALANCED WINDS

NON-DIVERGENT WINDS

NON-DIVERGENT STREAM FUNCTIONS

COMPARISON OF NON-DIVERGENT WINDS

PRIMITIVE EQUATION FORECASTS

GEOSTROPHIC VERSUS BALANCED WINDS

—

thesB8092345

A comparison of four non-divergent wind

DUDLEY KNOX LIBRARY



3 2768 00417082 9

DUDLEY KNOX LIBRARY